Universidade de Aveiro
Ano 2012

Secção Autónoma de Ciências da Saúde

MARIANA ISABEL GONÇALVES CORREIA

GENETIC CHARACTERIZATION OF NAD BIOSYNTHESIS ENZYMES IN HUMAN TUMOR CELL LINES

CARATERIZAÇÃO DE ENZIMAS DE SÍNTESE DO NAD EM CÉLULAS TUMORAIS HUMANAS

Universidade de Aveiro
Ano 2012

Secção Autónoma de Ciências da Saúde

MARIANA ISABEL GONÇALVES CORREIA

GENETIC CHARACTERIZATION OF NAD BIOSYNTHESIS ENZYMES IN HUMAN TUMOR CELL LINES

CARATERIZAÇÃO DE ENZIMAS DE SÍNTESE DO NAD EM CÉLULAS TUMORAIS HUMANAS

Dissertação apresentada à Universidade de Aveiro para cumprimento dos requisitos necessários à obtenção do grau de Mestre em Biomedicina Molecular, realizada sob a orientação científica da Doutora Raquel Monteiro Marques da Silva, Investigadora no Instituto de Patologia e Imunologia da Universidade do Porto, IPATIMUP.

Esta dissertação contou com o apoio do Instituto de Patologia e Imunologia Molecular de Universidade do Porto (IPATIMUP) e foi financiado por Fundos Nacionais através da FCT – Fundação para a Ciência e a Tecnologia no âmbito do projeto «PTDC/BIA-PRO/099888/2008».

o júri

presidente

Prof. Doutora Odete Abreu Beirão da Cruz e Silva,
Professora Auxiliar Com Agregação na Universidade de Aveiro

Doutora Isabel Alexandra Marcos Miranda
Investigadora na Faculdade de Medicina da Universidade do Porto

Doutora Raquel Monteiro Marques da Silva
Investigadora no Instituto de Patologia e Imunologia da Universidade do Porto (IPATIMUP)

Prof. Doutora Ana Gabriela da Silva Cavaleiro Henriques
Professora auxiliar convidada da Secção Autónoma das Ciências da Saúde da Universidade de Aveiro

agradecimentos

À minha mãe por ser Mãe, melhor amiga, confidente, um exemplo a seguir e o meu maior porto de abrigo. Obrigada por me veres sempre em voos muito altos. Devo-te tudo o que sou hoje!

À estrela maior que brilha todos os dias no céu. Sei que me segues e proteges todos os dias da minha vida.

Ao meu irmão, por querer sempre o melhor para mim.

À minha Matilde, por despertar todos os dias a eterna criança que há em mim.

Ao Nuno Venâncio, por ser o meu confidente e amigo de todos os dias, por ser o meu saco de boxe, mesmo quando não merece. Por saber quem eu sou, por me fazer sorrir e levantar o ânimo e por me deixar chorar, quando é preciso.

À Drª Raquel Silva, pela ajuda, pela paciência e por me ter ensinado bastante.

À Sara Pereira, por ter sido a uma grande mentora. Obrigada!

À Manuela Oliveira, pela ajuda incansável nesta fase derradeira e por ser a companheira das minhas pausas.

Ao João e Avó Mena por serem simplesmente pessoas importantes no meu crescimento.

À Catarina e à Cristina, por saber que posso contar sempre com vocês.

palavras-chave

NAD, vias de síntese do NAD, NAMPT, NAPRT, linhas celulares tumorais

resumo

Nicotinamida Adenina Dinucleótido (NAD) é um importante cofator nas reações metabólicas, sendo um substrato para as enzimas consumidoras de NAD, como as PARPs e as Sirtuinas. A via de síntese do NAD processa-se pela via *de novo,* na qual o NAD é sintetizado através do triptofano e do aspartato, e a via de reciclagem, onde o NAD pode ser reciclado a partir de diferentes precursores. As células cancerígenas têm necessidades aumentadas de NAD, pelo que inibidores da nicotinamida fosforibosiltransferase (NAMPT), a enzima mais importante na via de reciclagem do NAD nos humanos, estão em testes clínicos como agentes terapêuticos para o cancro. Contudo, apesar de serem agentes promissores, apresentam alguma citotoxicidade que pode ser ultrapassada pela adição de ácido nicotínico (NA) que vai ativar o ácido nicotínico fosforibosiltransferase (NAPRT) como via alternativa de síntese do NAD. Contudo, existe pouca informação acerca dos padrões de expressão do NAPRT, apesar de que é um biomarcador para a utilização do ácido nicotínico no tratamento com inibidores do NAMPT.

Assim, o grande objetivo deste trabalho é caracterizar as duas enzimas mais importantes da via de reciclagem do NAD, NAMPT e NAPRT, em linhas celulares tumorais humanas, integrando informação obtida através do ADN, ARN e proteína. Foram pesquisadas mutações e diferenças de expressão, sendo também feita a análise da estrutura 3D da proteína NAMPT-like, destacando três substituições de aminoácidos.

keywords **NAD, NAD biosynthesis pathways, NAMPT, NAPRT, tumoral cell lines**

abstract

Nicotinamide Adenine Dinucleotide (NAD) is a major cofactor in metabolic reactions, and is also the substrate of NAD-consuming enzymes such as PARPs and Sirtuins. NAD biosynthesis occurs via the *de novo* pathways, in which NAD is synthesized from tryptophan or aspartate, and the salvage pathways, where NAD can be recycled from several different precursors. Cancer cells have increased NAD requirements, thus inhibitors of nicotinamide phosphoribosyltransferase (NAMPT), the main human NAD salvage enzyme, are currently in clinical trials as novel cancer therapeutic agents. The citotoxicity presented by these inhibitors can be decreased by the use of nicotinic acid (NA) that will activate nicotinic acid phosphoribosyltransferase (NAPRT) as an alternative NAD synthesis pathway. Thus, the expression of NAPRT is a biomarker for the use of nicotinic acid as a chemoprotector in treatment with NAMPT inhibitors, however, few studies have addressed NAPRT expression in tumors.

So the main goal of this work was to characterize the two main enzymes involved in the NAD salvage pathways, NAMPT and NAPRT, in human tumor cell lines, by integrating data obtained from the three levels of biological information – DNA, RNA and proteins. Mutations and differences in expression levels were pursued and the analysis of the 3D structure of the NAMPT-like protein was also a goal, highlighting the impact of three amino acid substitutions.

INDEX

FIGURE INDEX

TABLE INDEX

ABBREVIATIONS

- **3' UTR –** three prime untranslated region
- **3HAO -** 3-Hydroxy-anthranilate 3,4-dioxygenase
- **ADP –** Adenosine diphosphate
- **AFMID –** Arylformamidase
- **APS -** Ammonium Persulfate
- **ART –** ADP-ribose transferases
- **ASO –** L-aspartate oxidase
- **ATP –** Adenosine triphosphate
- **cDNA –** Complementary Deoxyribonucleic Acid
- **CHAPS -** 3-[(3-cholamidopropyl)dimethylammonio]-1-propanesulfonate
- **CR** - Calorie restriction
- **DNA –** Deoxyribonucleic Acid
- **DTT –** Dithiothreitol

- **HDAC** - Histone deacetylase
- **IDO -** Indoleamine 2,3-dioxygenase
- **KMO** - Kynurenine 3-monooxygenase
- **KYNU –** Kynureninase
- **MMLV-RT –** Moloney Murine Leukemia Virus Reverse Transcriptase
- **mRNA –** messenger RNA
- **NA** – Nicotinic acid
- **NaAD –** Nicotinate adenine dinucleotide
- **NAD –** Nicotinamide Adenine Dinucleotide
- **NADH –** Reduced Nicotinamide Adenine Dinucleotide
- **NADP –** Phosphorylated Nicotinamide Adenine Dinucleotide
- **NADPH –** Reduced Phosphorylated Nicotinamide Adenine Dinucleotide
- **NAM** – Nicotinamide
- **NAMase** – Nicotinamidase
- **NaMN** – NA mononucleotide
- **NAMPT** – Nam phosphoribosyltransferase
- **NAPRT** – NA phosphoribosyltransferase
- **NMD –** Nonsense mediated decay
- **NMN** – Nicotinamide mononucleotide
- **NMNAT** - Nicotinate/nicotinamide mononucleotide adenyltransferase
- **NR -** Nicotinamide riboside
- **NRK -** Nicotinamide riboside kinases
- **NS -** NAD-synthetase
- **PAGE –**Polyacrylamide Gel Electrophoresis
- **PARP -** Poly-ADP-ribose polymerase
- **PBEF 1**- Pre-B-cell-enhancing factor 1
- **PBEF 2**- Pre-B-cell-enhancing factor 2
- **PCR:** Polymerase Chain Reaction
- **PRPP – 5'-** Phosphoribosyl – 1' - pyrophosphate
- **PTC –** premature termination codons
- **QPT -** Quinolinate phosphoribosyltransferase
- **QS –** Quinolinate Synthetase

- **RNA –** Ribonucleic acid
- **RT-PCR** - Reverse Transcriptase Polymerase Chain Reaction
- **SDS** - Sodium Dodecyl Sulphate
- **SIR2 -** Yeast silent information regulator 2
- **SIRT –** Sirtuin
- **TBE –** Tris-borate-EDTA
- **TDO -** Tryptophan 2,3-dioxygenase
- **TEMED -** Tetramethylethylenediamine
- **TGM –** Tris-Cl, Glycine, Methanol

INTRODUCTION

1. NAD and NAD-dependent reactions

Nicotinamide Adenine Dinucleotide (NAD^+) and its reduced and phosphorylated forms (NADH, $NADP^+$, and NADPH), have pivotal roles in a wide number of cellular tasks, being involved in metabolism, energy production and cell regulation in all organisms [1-6].

NAD is involved in redox and non-redox reactions. In the redox reactions, which consist in the transfer of electrons between substrates, this coenzyme switches between its oxidized and reduced forms, contrary to the non-redox reactions, where NAD is consumed by a group of enzymes. The transfer of electrons in redox reactions is essential to cells as they are part of the glycolysis/citric acid cycle and are involved in regeneration of ATP from ADP. Both the oxidized and the reduced forms of NAD, (NAD^+/NADH) are used in the redox reactions, and because they are also consumed in several reactions the cell must maintain high concentrations of NAD [1-6]. Enzymes

that use NAD as a substrate act as metabolic regulators and sensors in the cell that can regulate downstream metabolic pathways [2].

NAD^+ consuming enzymes break down NAD^+ and are divided into three groups. The first group includes **ADP-ribose transferases (ARTs)** and **poly-ADP-ribose polymerases (PARPs)**, which transfer and/or polymerize NAD^+-derived ADP-ribose, acting like a post-translational modification [7]. The second group consists of **cADP-ribose synthases** that are important in intracellular calcium signaling ([8] and reviewed in [2]). The third class of enzymes are the **sirtuins** - a group of NAD^+ -dependent deacetylases that remove acetyl groups from lysine residues on target substrates such as histones and microtubules [9].

One example of NAD-consuming reaction is ADP-ribosylation, where the addition of ADP-ribose moieties to proteins occur. This reaction involves either the addition of a single ADP-ribose moiety, in a reaction called mono-ADP-ribosylation by ARTs, or the transfer of ADP-ribose to proteins in long branched chains – poly-ADP-ribosylation by PARPs.

PARPs, a superfamily of proteins related to a number of cellular processes, are involved in maintenance of chromatin structure, DNA repair and programmed cell death. Of all the members, PARP1 and PARP2 have been the most widely studied because they participate in almost all the PARP activity in the cell [2-3, 7, 10-11].

Moreover, poly-ADP-ribosylation represents an immediate response to genotoxic damage caused by oxidative stress, alkylating agents or ionizing radiation. PARP-1 binds to DNA strand breaks and cleaves NAD^+ into nicotinamide and ADP-ribose, polymerizing the last one onto nuclear acceptor proteins, like histones, transcription factors and PARP itself. This process (adding units of ADP-ribose) is a post-translational modification that can help DNA repair and plays, therefore, a protective role in response to moderate genotoxic insult [3, 11]. However, when a cell has high levels of DNA damage it can trigger an uncontrolled PARP-1 activity, which may lead to an excessive depletion of intracellular NAD concentrations, decreasing resistance to stress and culminating in cell death [3]. Therefore, maintenance of NAD levels is of paramount importance for cellular function and survival. In fact, PARP-1 has two major roles: promoting DNA repair in cases of mild DNA damage and triggering cell death in response to excessive genotoxic insult. These two actions

represent a probable mechanism that can limit the accumulation of cells containing heritable genetic errors [3].

Due to its roles in cell death, there are studies demonstrating that PARP inhibitors protect against cardiac, inflammatory and neurodegenerative conditions. These inhibitors are also being considered for cancer treatment, as cancer cells have increased demands for DNA repair proteins [5, 10].

Another important NAD role is as a precursor of cyclic ADP-ribose, which is produced by cADP-ribose synthases and that acts in calcium signaling by releasing calcium from intracellular stores [2, 12]. cADP-ribose synthases are also known as lymphocyte antigens CD38 and CD157 that were originated by gene duplication and are highly conserved in most eukaryotes [2, 12]. These two enzymes are multifunctional enzymes that use NAD+ as a substrate to generate second messengers, like cADP-ribose, that mediates the calcium mobilization [2, 8, 12].

The third class of NAD^+ consuming enzymes is sirtuins, a family of NAD^+ dependent protein deacetylases that are involved in transcriptional regulation by deacetylating histones and by the alteration of nucleosome structure. Sirtuins are class III protein deacetylases, and are the only histones deacetylases (HDACs) that require NAD for their enzymatic activity [3-4, 13-15]. These enzymes are highly conserved from bacteria to humans and yeast SIR2 (silent information regulator 2), the founding member of the sirtuin family, was originally shown to extend lifespan in the budding yeast [16] and invertebrates, like flies [17] and worms [18].

In mammals, there are seven described homologs of yeast SIR2, named SIRT1 to SIRT7. This great variety of sirtuin genes has been justified by the different localizations of the proteins that they encode and their different substrates and biological functions (Table 1).

SIRT1 is the best characterized mammalian sirtuin, so far. In general, SIRT1 is activated in situations of energy stress, such as fasting, exercise or low glucose availability. Of great importance is the fact that SIRT1 regulates the activity of a number of transcription factors and co-factors by modulating their acetylation status [2, 14-15].

SIRT1 was also found to have dual functions as an oncogene and as a tumor suppressor. Sirtuin deacetylates lysine residue 383 of p53, therefore, it acts as an oncogene by repressing p53 transcriptional activity [14]. p53 is a tumor suppressor,

with anti-proliferative effects, such as growth arrest, apoptosis and cell senescence [19]. So the down-regulation of p53 activity by SIRT1 can lead cell to tumorigenesis [19]. Moreover, SIRT1 was found to be overexpressed in leukemia, glioblastoma, prostate, colorectal or skin cancer [14, 20-22].

Table 1 - Activity, sub-cellular localization and function of the different sirtuins. In [15]

Name	Activity	Sub-cellular Location	Function
SIRT1	Deacetylase	Nucleus	Cell survival/metabolism
SIRT2	Deacetylase	Cytosol	Cell cycle
SIRT3	Deacetylase	Mitochondria	Thermogenesis/metabolism
SIRT4	ADP-ribose-transferase	Mitochondria	Insulin secretion/metabolism
SIRT5	Deacetylase	Mitochondria	unknown
SIRT6	ADP-ribose-transferase	Nucleus	DNA repair
SIRT7	unknown	Nucleolus	rDNA transcription

Contrary, SIRT1 can act as a potential tumor suppressor however the exact molecular effects of SIRT1 might vary according to the tissues and/or cancer types [14, 20-22]. For example, SIRT1 was able to suppress intestinal tumorigenesis and colon cancer growth in a β-catenin-driven mouse model of colon cancer. Deacetylation of β-catenin leaded to its cytoplasmic localization, instead of the normal nuclear localization, leading to a reduced colon cancer tumor formation and proliferation [1, 23-24].

2. NAD biosynthesis pathways

NAD^+ can be synthesized by different pathways, the *de novo* (from amino acids) and the salvage pathways (from metabolites) (figure 1). The *de novo* pathways start with the amino acid aspartate (in bacteria and plants) or tryptophan (bacteria, fungi and animals) while the salvage pathways start with nicotinamide (NAM), nicotinic acid (NA) or their ribosides [1, 20, 25].

In the *de novo* pathway from tryptophan (figure 1, in green) quinolinate is synthesized, by the action of six enzymes: tryptophan 2,3-dioxygenase (TDO); Indoleamine 2,3-dioxygenase (IDO); Arylformamidase (AFMID); kynurenine 3-

monooxygenase (KMO); kynureninase (KYNU) and 3-Hydroxy-anthranilate 3,4-dioxygenase (3HAO). In the aspartate pathway (represented in black in figure 1) iminoaspartate is synthesized from L-aspartate through the activity of the ASO enzyme. Iminoaspartate is converted in Quinolinate (QA) by quinolinate synthetase (QS). Next, by the action of Quinolinate phosphoribosyltransferase (QPT), quinolinate is condensed with 5-phospho-α-D-ribose 1-diphosphate to form NA mononucleotide (NAMN). After, the reactions are common between the *de novo* and salvage pathways (figure 1, in red) [1-2, 25-26]. NAMN is adenylylated to Nicotinate adenine dinucleotide (NaAD) by action of nicotinate/nicotinamide mononucleotide adenyltransferase (NMNAT). NAD-synthetase (NS) then converts NaAD into NAD^+ [20, 27].

Although NAD^+ can be synthesized *de novo*, it is assumed that the main source of NAD^+ in the human cells is the salvage pathway which requires the uptake of NAD^+ precursors from the diet [2].

In the two-step salvage pathway (figure 1, in blue), nicotinamide (NAM) and PRPP (5′-phosphoribosyl-1′-pyrophosphate) produces Nicotinamide Mononucleotide (NMN) by the action of Nicotinamide phosphorybosyltransferase (NAMPT – the rate limiting step of this part of the pathway) [20]. NMN is converted to NAD^+, by action of NMNAT [20].

The purple and red part of figure 1 represents the four-step salvage pathway.

Nicotinic acid is produced from nicotinamide (NAM) by nicotinamidase (NAMse). Next, the nicotinic acid (NA) and PRPP are phosphoribosylated to NaMN by the enzyme NAPRT, which is adenylylated to NaAD and amidated to form NAD (this is the Preiss-Handler pathway) [1-2, 25-26]. Because mammals lack nicotinamidase, NA seems to arise, primarily, from extracellular sources, directly from the diet or, indirectly, from dietary NAM after deamidation by gut flora deamidase [28].

The orange part of figure 1 represents an alternative NAD salvage pathway, found recently to be present in yeast and humans. Nicotinamide riboside (NR), a natural product present in milk is converted to NAD^+ through the action of conserved eukaryotic NR kinases [25, 27, 29].

Introduction

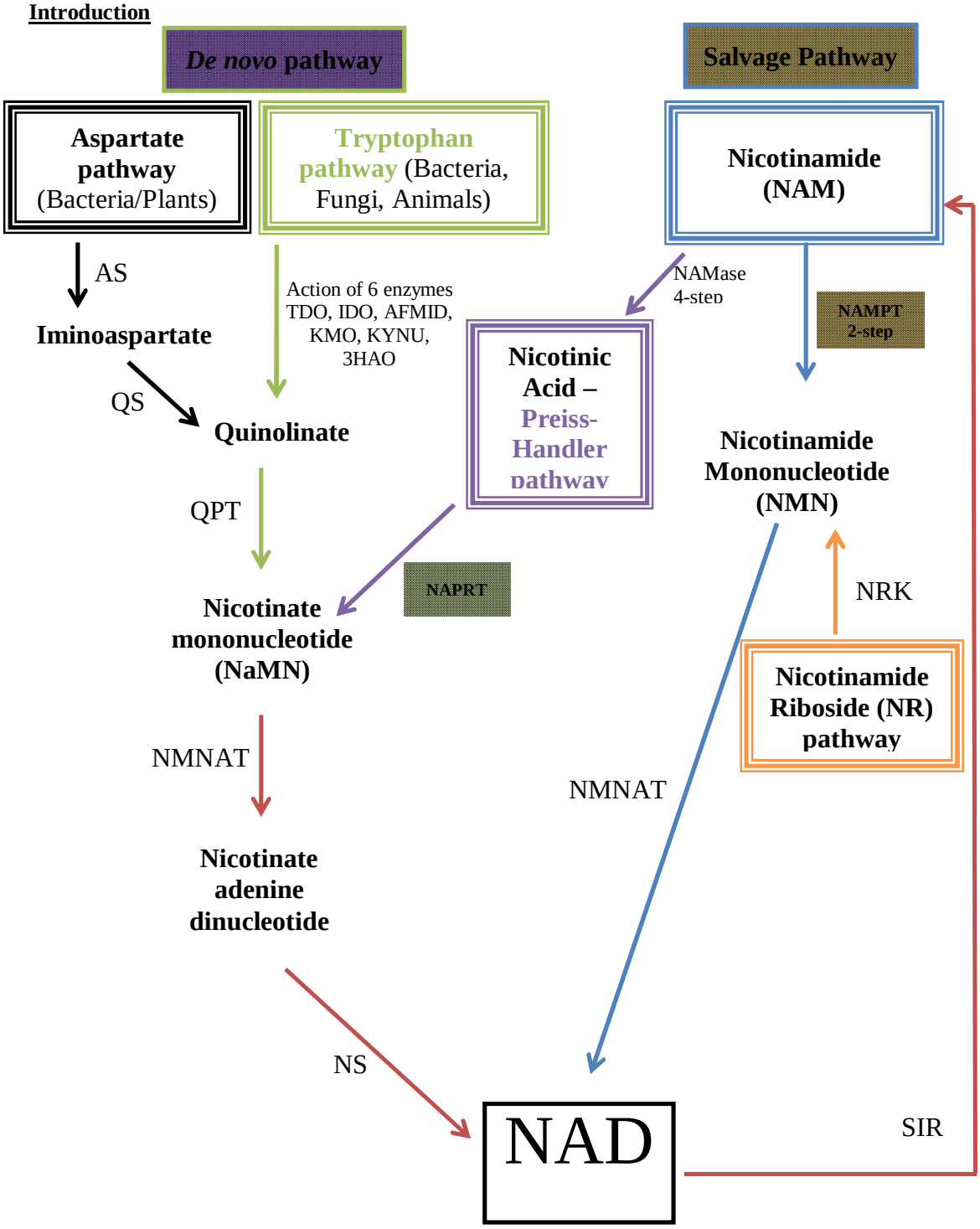

Figure 1 - The biosynthetic pathways of nicotinamide adenine dinucleotide (NAD+). The green and black arrows indicate steps specific to the *de novo* pathway; red arrows indicate steps shared by the *de novo* and salvage pathways; the blue, purple and orange arrows represent the salvage pathways. Abbreviations: ASO, L-aspartate oxidase; QS, Quinolinate synthetase; QPT, Quinolinate phosphoribosyltransferase; NMNAT, nicotinate/nicotinamide mononucleotide adenyltransferase; NS, NAD-synthetase; TDO, Tryptophan 2,3-dioxygenase; IDO, Indoleamine 2,3-dioxygenase; AFMID, Arylformamidase; KMO, kynurenine 3-monooxygenase; KYNU, kynureninase; 3HAO, 3-Hydroxy-anthranilate 3,4-dioxygenase; NAMase, nicotinamidade; SIRT, silent information regulator; NRK- nicotinamide riboside kinase; NAMPT, nicotinamide phosphorybosyltransferase; NAPRT, nicotinic acid phosphorybosyltransferase.
(adapted from [1] and [2])

Introduction

As there are different pathways to synthesize NAD, the question of substrate preference for NAD biosynthesis is yet unsolved [2]. Moreover, organisms contain all the enzymes required for more than one pathway suggesting that differential pathway usage could be explained by the localization of the enzymes, because some of them are strictly confined to a limited number of organs [2]. In mammals, the 2-step salvage from nicotinamide is essential and used predominantly [1].

NAMPT and NAPRT are two important enzymes involved in NAD metabolism, and are the main focus of this work. NAMPT constitutes the rate limiting step in the NAD+ salvage pathway from nicotinamide, and NAPRT, the intersection point between the salvage and the *de novo* pathways, allows the use of nicotinic acid to produce NAD.

3. NAMPT and NAPRT

NAMPT regulates several metabolic and stress responses, as a major NAD biosynthetic enzyme but also by removing nicotinamide that inhibits the activity of NAD-consuming enzymes [11, 19, 30].

NAMPT was first described as a pre-B-cell-enhancing factor (PBEF) and over the years, accumulated evidence indicates that it is a pleiotropic protein acting as a growth factor, a cytokine, and an enzyme. Also, recent findings showed that NAMPT plays a central role in controlling the circadian clock machinery, by dictating the periodical oscillations of some of its key transcription factors [31-32].

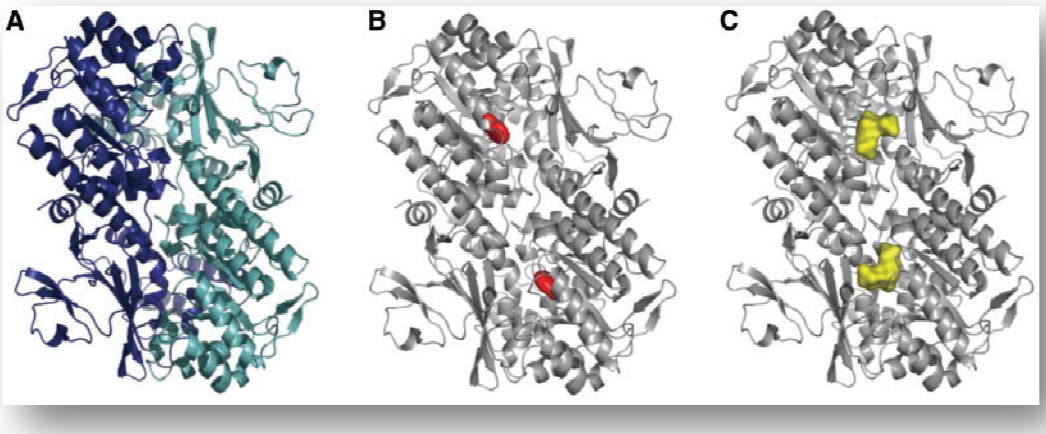

Figure 2 - The crystal structures of human NAMPT. Each subunit is distinguished by dark and light blue (A). In (B) is represented the complex with NM and in (C) with PRPP. In [33]

Introduction

The protein structure has been determined and shows that it belongs to a dimeric class of type II phosphoribosyltransferases (figure 2) [4, 33-34].

In mammals, NAMPT is present in intracellular (cytoplasm) and extracellular forms (iNAMPT and eNAMPT, respectively). The function of iNAMPT as a NAD biosynthetic enzyme has been firmly supported by the studies involving its biochemical and structural properties, and its expression is induced by a variety of cellular stresses and nutrient restriction [35]. Contrary, the role and function of eNAMPT has not been definitively elucidated. It is thought that eNAMPT induces leukocyte adhesion to endothelial cells by activating intercellular adhesion molecule-1 indicating that eNAMPT has a potential role in the pathogenesis of vascular inflammation in Obesity and Type 2 Diabetes Mellitus [4, 35-36].

The human NAMPT gene is localized in chromosome 7 (7q22.2) and has a length of 36,908 bp. The gene is composed of 11 exons and NAMPT reference coding sequence has a total length of 1476 bp, which encodes 491 amino acids [37]. Additional transcripts are predicted according to EnsEMBL, which are presented in the table 2 identifying their names, sizes, and molecular mass and size of the corresponding encoded protein.

Table 2 - Predicted NAMPT transcripts. Data retrieved from EnsEMBL, release 67 (May 2012) (http://www.EnsEMBL.org/Homo_sapiens/Transcript/Summary?g=ENSG00000105835;r=7:105888731-105925638;t=ENST00000222553)

Name	Size (bp)	Molecular Mass (kDa)	Size (aa)
NAMPT 001	4582	55.5	491
NAMPT 002	1213	41.9	368
NAMPT 003	1147	10.5	88
NAMPT 004	300	7.2	60

NAMPT is also predicted to have a pseudogene – NAMPT-L (nicotinamide phosphoribosyltransferase-like), also known as pre-B-cell colony enhancing factor 2 (PBEF 2) that is localized in chromosome 10 (10p11.21).

NAPRT catalyzes the conversion of nicotinic acid to nicotinate mononucleotide [1] and is conserved in prokaryotes, archaea and eukaryotes, indicating the ubiquitous nature of the Preiss-Handler pathway [28].

Introduction

Through the activity of NAPRT, nicotinic acid is more effective in increasing NAD levels in human cells than nicotinamide, although nicotinamide levels are much higher than nicotinic acid levels [28, 38]. In mice, some tissues, like heart, kidney and red blood cells, where NAPRT was found to be more expressed, could preferentially use the NAD salvage pathway from nicotinic acid [28, 38]. NAPRT, unlike NAMPT, is not subjected to feedback inhibition by the physiological concentration of NAD [28, 38]. Insensitivity could allow NA to elevate NAD levels beyond the basal levels [38]. Therefore, both precursors are relevant for NAD^+ biosynthesis, possibly with distinct and complementary roles in different cells.

Human NAPRT gene is localized in chromosome 8 (8q24.3) having a total length of 3559 bp, with its coding sequence presenting a total length of 1617 bp and a total of 13 exons. Like NAMPT, NAPRT protein has a predicted dimeric organization (figure 3) being present in cytosol [38].

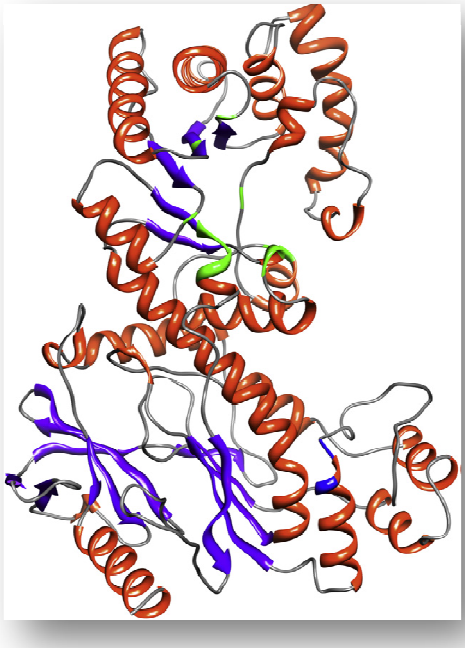

Figure 3 - Predicted 3D-structure of human NAPRT, in [28]. The α-helices are in orange, β-sheets in purple and loops are in grey, being residues of the active site shown in green.

The predicted 3D-structure of human NAPRT resemble the architecture of the QPTs, which would classify it as a type II phosphoribosyltransferase [39].

Additional transcripts are predicted, which are presented in the table 3 identifying their names, sizes and molecular mass size of the corresponding encoded protein.

Table 3 - Predicted NAPRT transcripts. Data retrieved from EnsEMBL, release 67 (May 2012) http://www.EnsEMBL.org/Homo_sapiens/Gene/Summary?g=ENSG00000147813;r=8:144656955-144660819

Name	Size (bp)	Molecular Mass (kDa)	Size (aa)
NAPRT-001	1774	62.2	584
NAPRT-002	1965	57.6	538
NAPRT-003	1654	56.1	525
NAPRT-004	1877	52.2	490
NAPRT-201	1721	60.2	566

4. NAMPT and NAPRT- based anti-tumoral therapies

The hallmark of cancer cells is the chronic uncontrolled cell proliferation involving higher demands of energy in order to fulfil their cell growth and division needs. In fact, cancer cells have a dysregulated metabolism, with increased energy consumption and DNA repair [40-41].

In normal cells, where oxidative phosphorylation takes place, each glucose molecule produces 38 ATP molecules, whereas in glycolysis only 2 ATP and 2 NADH molecules are produced from a glucose molecule [40-41].

Cancer cells, even in the presence of sufficient oxygen to undergo mitochondrial oxidative phosphorylation, upregulate glycolysis (in a phenomenon known as “Warburg effect”). This is inefficient in producing ATP however it ensures tumor cell survival and the advantage that this iconic “Warburg effect” confers to cancer cells is not determined yet (reviewed in [42]).

NAMPT was found to be overexpressed in some human cancers, like astrocytomas/glioblastomas [43], human malignant lymphomas [44], ovarian [45] and colorectal tumors [46]. Thus, several groups developed inhibitors of NAMPT, like FK866, CHS828, APO866 and the CHS828 prodrug EB1627/GMX1777 as anti-tumor agents [4, 32, 40, 47-48]. Although being promising cancer drugs currently in clinical trials, these drugs exhibit citotoxicity, which might be attributable to two processes.

Introduction

First, being a NAMPT-inhibitor, these drugs reduce intracellular NAD^+, decreasing the activities of prosurvival enzymes that use NAD^+ as a substrate. Second, NAMPT inhibition leads to accumulation of intracellular nicotinamide, an endogenous inhibitor of some NAD^+ - consuming enzymes, like PARPs and sirtuins, thereby interfering with DNA repair and cell survival, leading to citotoxicity [40].

Cells rely on the more readily available nicotinamide pathway for NAD biosynthesis, which can culminate in apoptosis after NAMPT inhibiton, however, cells that have the ability to use the nicotinic acid pathway for NAD synthesis remain unaffected [48]. Due to this fact, the citotoxicity manifested by these novel anticancer drugs can be overcomed by adding NA, which may replenish NAD^+, via NAPRT, in the treatment of tumors that are deficient in NAPRT. Thus, the expression of NAPRT is a biomarker for the use of nicotinic acid as a chemoprotector in treatment with NAMPT inhibitors, however, a few studies have addressed NAPRT expression in tumors.

In this work, we have performed a genetic screen with the objective to identify novel inactivating mutations and characterize the expression profile of both NAMPT and NAPRT in several human tumor cell lines.

AIM OF THE STUDY

Characterization of two main enzymes involved in the NAD salvage pathways, NAMPT and NAPRT, in human tumor cells lines, by integrating data obtained from the three levels of biological information – DNA, RNA and proteins. For this, detection of mutations, differences in expression levels and the analysis of the 3D structure of the NAMPT-like protein, highlighting the impact of three amino acid substitutions, were pursued.

MATERIALS AND METHODS

Cell lines

For this thesis several human tumoral cell lines and one embryonic cell line were used, obtained from distinct tissues. Most of the cell lines were obtained from the IPATIMUP Cell Lines Bank and are described in table 4.

C643 cell line was obtained from Prof. Marc Mareel (Laboratory of Experimental Cancerology, Ghent University Hospital,Ghent, Belgium). Mel 202 was kindly obtained from Dr. M.J. Jager, LUMC, Leiden, The Netherlands being established by Dr. B.R. Ksander, Schepens Eye Research Institute, Boston, USA.

Materials and Methods

Table 4 - Cell lines used with description of the tissue of origin, type of the cell line, source and a reference

Cell line	Tissue	Type	Source	Reference
786-O	Kidney	Renal Adenocarcinoma	Male	ref. ATCC nr. CRL-1932
C643	Thyroid	Thyroid Carcinoma	Unknown	Obtained from Prof. Marc Mareel [49]
Mel 202	Uvea	Uveal Melanoma	Unknown	Dr. M.J. Jager, LUMC, Leiden, The Netherlands
DLD-1	Colon	Colorectal Adenocarcinoma	Male	[50] ref. ATCC nr. CCL-221
HUVEC-C	Umbilical vein	Embryonic Normal Vascular Endothelium	Unknown	[51] ref. ATCC nr. CRL-1730
Hela	Cervix	Cervical Adenocarcinoma	Female	ref. ATCC nr. CCL-2
NB-4	Bone marrow	Promyelocytic Leukemia	Unknown	[52]
HL-60	Peripheral blood	Promyelocytic Leukemia	Female	[53] ref. ATCC nr. CCL-240
HCT-15	Colon	Colorectal Adenocarcinoma	Male	[50] ref. ATCC nr. CCL-225
A549	Lung	Pulmonary Adenocarcinoma Adenocarcinoma	Unknown	ref. ATCC nr. CCL-185

DNA, RNA and Protein Extraction

Materials and Methods

Extractions were performed with the Illustra TriplePrep Kit (GE Healthcare).

This kit was designed for the rapid extraction of genomic DNA, total RNA and total denaturated protein from a single undivided sample. The first step of the extraction protocol consisted in sample homogenization and lysis. Then, the lysate was transferred to a column and centrifuged at 11000 x g for 1min. The flowthrough was saved for RNA and Protein extraction. The column was washed in successive steps with Lysis Buffer and Wash Buffer. The DNA elution was achieved adding Elution Buffer to the center of the column, followed by a centrifugation step at 11000 x g for 1min (figure 4).

For RNA isolation, a new column and collection tube were used. Absolute Acetone was added and this mixture was centrifuged for 1min at 11000 x g, saving the flowthrough for protein isolation. Next, DNAse Treatment was performed by addition of DNAse type I to the samples and incubating for 10min at room temperature. The column was washed and the RNA eluted by centrifugation at 11000 x g for 1min. (figure 4).

Protein Precipitation Buffer was added to the previously saved flowthrough and centrifuged at 16000 x g for 10min, and the supernatant was removed. The protein pellet was washed with distilled water, centrifuged at 16000 x g for 10min and the supernatant was removed. Finally, the protein pellet was ressuspended in sample buffer containing 8M urea, 2% CHAPS (3-[(3-cholamidopropyl)dimethylammonio]-1-propanesulfonate) and 50mM DTT (Dithiothreitol) (figure 4).

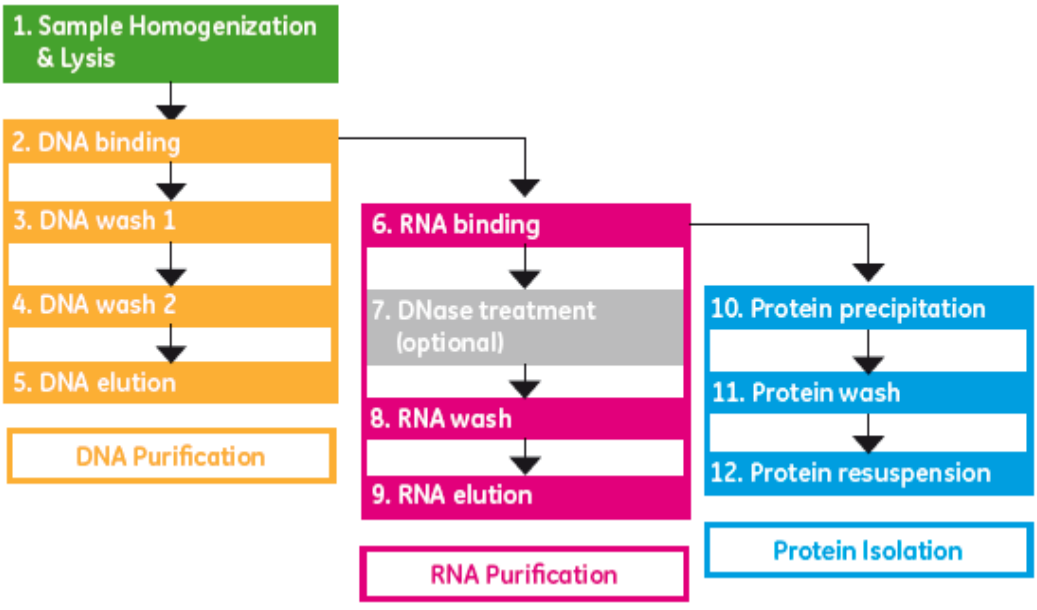

Figure 4 - Schematic representation of the Illustra TriplePrep Kit

All the samples were quantified by measuring the absorbance using a NanoDrop.

RNA Purification

In order to eliminate DNA contamination in the cDNA preparations, RNA was treated with DNase I, RNase-free (Fermentas Life Sciences). DNase I, RNase-free, is a 29kDa endonuclease that hydrolizes phosphodiester bonds in the single and double-stranded DNA producing mono and oligodeoxyribonucleotides.

In a RNase free-tube, RNA (1-2µg), 10x reaction buffer with $MgCl_2$ (1µL), water (to 9µL) and DNase I, RNase-free (1-2µL) were added. This mixture was incubated at 37ºC for 30min. Next, 1µL 25mM EDTA was added and incubated at 65ºC for 10min.

cDNA preparation

cDNA was obtained by RT-PCR – Reverse Transcriptase Polymerase Chain Reaction, in which RNA strand is reversely transcribed into its DNA complement, using the RETROscript® Kit (Ambion). For this, 1–2µg total RNA, 2µL Oligo(dT) and Nuclease-free Water were added to a final volume of 12µL. This mixture was heated for 3min at 85ºC, adding then 2µL 10x RT buffer, 4µL dNTP mix, 1µL RNase Inhibitor and 1 µL MMLV-RT, for a final volume of 20µL. This last mixture was incubated for 1hour at 42ºC and then, for 10 min at 92ºC, in order to inactivate the reverse transcriptase. cDNA was further used for PCR amplification.

PCR Amplification

Samples were amplified using PCR (polymerase chain reaction). Primers and target regions are indicated in table 5.

Materials and Methods

Human NAMPT gene fragments were amplified using 5µL MasterMixHotStarTaq (Qiagen), 1µL of primer forward (2µM), 1µL of primer reverse (2µM), 2µL of ddH_2O and 1µL of DNA.

The amplification of fragments corresponding to exon 2, 7 and 9 was performed with the following cycling parameters: an initial denaturation step at 95ºC for 15min; 35 cycles consisting of 30sec at 94ºC, 30sec at 58ºC and 30sec at 72ºC followed by a final extension step at 72ºC for 10min. For exons 4 and 8, similar conditions were used, but with an annealing temperature of 60ºC. Different conditions were used for intron 4: 95ºC for 15min was used for the initial denaturation, 35 cycles consisting of 30sec at 95ºC, 1min ate 52ºC and 1min at 72ºC followed by a final extension step at 72ºC for 10min.

To amplify both exon 4 and intron 4 Hs_NAMPT_ex4F and Hs_NAMPT_in4R were used with a PCR protocol as described: 95ºC for 15min was used for the initial denaturation, 35 cycles consisting of 30sec and 95ºC, 1min at 54ºC and 1min at 72ºC followed by a final extension step at 72ºC for 10min. Samples 3 and 10 failed to amplify with this protocol, so 1µL of Water was replaced by 1µL of Q solution.

To amplify NAMPT cDNA, a mixture with 5µL of MasterMixHotStarTaq (Qiagen), 1µL Q solution (Qiagen), 1µL of primer forward (2µM), 1µL of primer reverse (2µM), 1µL of ddH_2O and 1µL of DNA was used.

The PCR consisted of the following steps: an initial denaturation step at 95ºC for 15min; 35cycles consisting of 30sec at 95ºC, 1min at 58ºC and 1min at 72ºC followed by a final extension step at 72ºC for 10min.

PCR for NAPRT gene fragments is prepared with 5µL MasterMixMultiplexQiagen (Qiagen) and 1µL Q solution (Qiagen), plus 1µL of primer forward (2µM), 1µL of primer reverse (2µM), 1µL of ddH_2O and 1µL of DNA, to a total volume of 10µL.

Amplification reactions of fragments use the following cycling parameters: an initial denaturation step at 95ºC for 15min; 35 cycles consisting of 30sec at 94ºC, 30sec at 61ºC and 30sec at 72ºC followed by a final extension step at 72ºC for 10min.

For the amplification of NAPRT cDNA, 5µL of MasterMixHotStarTaq (Qiagen), 1µL Q solution (Qiagen), 1µL of primer forward (2µM), 1µL of primer reverse (2µM), 1µL of ddH_2O and 1µL of DNA were used with the following cycling

Materials and Methods

parameters: an initial denaturation step at 95ºC for 15min; 30 cycles consisting of 30sec at 95ºC, 45sec at 60ºC and 1min at 72ºC followed by a final extension step at 72ºC for 10min.

After the PCR reactions, fragments were electrophoresed on acrylamide or agarose gel in order to test the amplification.

Table 5 - Primers used in this study

DNA	**NAMPT**	Exon 2	5'-CTTCAAGCCTTTTCTGTTGTG-3' (sense) and 5'-CTTAGAACATCAAACACACACC-3' (anti-sense)
		Exon 4	5'-AGCACGTGGCAGCATTAAAC-3' (sense) and 5'-GATGAGGAAATTGAAGCCTGG-3' (anti-sense)
		Exon 7	5'-CATAACAGCTTGGGGGAAAG-3' (sense) and 5'-CTCTCTCTGGGCTGCAACT-3' (anti-sense)
		Exon 9	5'-CAGTCTTGGATGCTTCATTC-3' (sense) and 5'-CTCCCTTCTTTCCTTGTTTCTG-3' (anti-sense)
		Intron 4	5'- AGGAAGGGTACATTTTGGGC-3'(sense) and 5'- AAACACCCTCTTGGACCTC-3'(anti-sense)
		Exon 8	5'- CCCTTTAAAGTACACTGGACC -3'(sense) and 5'- GTAAGTATGGCTTGGCTGGC -3'(anti-sense)
	NAPRT	Exon 2	5'-ACCTCTACCAGGCCACCATG-3' (sense) and 5'-CAGCCCACCTGGCGTAGC-3' (anti-sense)
		Exon 7	5'-CTACAGCGTGTGGAGGTGAG-3' (sense) and 5'-CACCTGTGCTCACCTTCTGC-3' (anti-sense)
cDNA	**NAMPT**	Exon 1-4	5'-CTCATTTTTCTCCTTCCTCGC-3' (sense) and 5'-TCCTCTGGGAATGACAAAGC-3' (anti-sense)
		Exon 3-7	5'-TCCAGGAAGCCAAAGATGTC-3' (sense) and 5'-CTTTCCCCCAAGCTGTTATG-3' (anti-sense)
		Exon 6-8	5'-GCATCTGCTCACTTGGTTAAC-3' (sense) and 5'- CTCTAAGATAAGGTGGCAGC-3' (anti-sense)
		Exon 7-11	5'-GGCACCACTAATAATCAGACC-3' (sense) and 5'-CAAACCCCACACATCTGTAC-3' (anti-sense)
	NAPRT	Exon 9-13	5' - GGCATTGGCACCAGTGTGGTCACCTG – 3'(sense) and 5' - GGGGGACTGCCCCGCACACA – 3' (anti-sense)

Gel electrophoresis

Electrophoresis is a technique used to separate and purify macromolecules that differ in size, charge or conformation. Proteins and nucleic acids are electrophoresed within a matrix or "gel".

The gel is composed of either agarose or polyacrylamide. Polyacrylamide is a cross-linked acrylamide polymer having a rather small range of separation, but very high resolving power. Agarose gels have a large range of separation, but relatively low resolving power.

The acrylamide gel (1x) were prepared with 3mL acrylamide T9C5 (National Diagnostics), 170µL APS (Promega) and 7µL TEMED (National Diagnostics). After acrylamide polymerization, the samples were added and resolved by horizontal electrophoresis in the Multiphor II system.

Samples were visualized by silver staining of the gels: 10min in ethanol followed by the addition of Nitric acid (1% for 5min) and a washing step with distilled water (2x10seg). Next, gels were immersed in Silver nitrate (0.2% for 20min), followed by a new wash with distilled water (2x10seg). Revelation was performed using a solution of Sodium carbonate with formaldehyde (4%) for a variable amount of time and, reaction was stopped with Acetic Acid (10%) followed by a new wash with distilled water.

Agarose gels of either 1% (120mL/300mL of TBE (Tris-borate-EDTA) buffer with 1.2g/3g of agarose, for small or large gels, respectively) or 1.5% (300mL of TBE buffer with 4.5g of agarose) were used. To visualize the DNA bands, GelRed solution was added to the gel solution.

In both acrylamide and agarose gel, the O'GeneRuler™ 100bp DNA Ladder Plus, ready-to-use was used (Fermentas – Life Sciences).

Sequencing

The amplified fragments were purified with ExoSap-IT (USB Corporation), to remove primers and unincorporated dNTPs. This step was performed using 2.5µL of

PCR product and 1µL of ExoSap-IT. The mixture was then submitted to two cycles of 15min, first at 37ºC and the second at 85ºC to inactivate the enzyme.

Sequencing reactions were performed using the BigDye® Terminator kit v3.1 (Applied BioSystems) with 1.5µL PCR product treated with ExoSap; 1µL H_2O; 0.5µL primer (2µM); 2µL BigDye® Terminator v3.1 (Applied BioSystems) and were subjected to 35 cycles under the following conditions: 96ºC for 20sec; 55ºC for 10sec; 60ºC for 1.5min. These cycles were preceded by an initial denaturation step of 96ºC for 5min and followed by a final extension step of 60ºC for 10min.

Products were cleaned with Sephadex™ (GE Healthcare) and run in an ABI PRISM 3130x1 (Applied Biosystems).

The subsequent analysis of the electropherogram data was performed with Geneious software, version 5.5.7. [54].

SDS-Page

Protein samples were run in a SDS-polyacrylamide gel electrophoresis (SDS-PAGE). This is a method where proteins are resolved in a semi-solid matrix, the polyacrylamide gel, based in their molecular weight. This is achieved by the addition of SDS, an anionic detergent that negatively charges the molecules to the same degree in proportion to their length. Under these conditions, the mobility of the molecules is relative to their size: light molecules migrate faster in the gel, while the migration of heavy molecules is slower.

Two acrylamide gels of 12.5% were prepared (one for Coomasie Blue staining and another for Western-Blot) using 3.2mL of water, 100 µL of SDS 10%, 3.75mL of Tris-Cl, 50µL of acrylamide 40% (29:1), 50µL of APS (10%) and 10µL of TEMED for the resolving gel. For the stacking gel 3.464mL of water, 50µL of SDS 10%, 1mL of Tris-Cl, 500µL of Acrylamide 40% (29:1), 50µL of APS 19% and 10µL of TEMED were used.

The samples were prepared by addition of 5µL of Laemmli Buffer (LB) to 5µL of sample, boiled (90ºC for 5min) and loaded into the gel. Gels were then run for 10min at 50V and for 60min at 120V. After running, gels were stained with Coomasie Blue or electroblotted as described below. For Coomassie Blue staining, gel was washed 3 times for 5min before staining with Comassie Blue for 60min.

Western-Blot

The Western-Blot is a technique used to detect proteins based on their ability to bind specific antibodies. It provides information about the presence, relative molecular weight and expression amount of a protein.

It is necessary to transfer the proteins from an electrophoresis gel to a solid support. In this experimental system, proteins were transferred to nitrocellulose membranes for 1 hour at 350mA and 100V. Gel and nitrocellulose membrane were first hydrated in TGM (Tris-Cl, Glycine and Methanol) (BIORAD) for 10min.

The next step was the rehydration of the membrane using 100mL TBS (15min), followed by the blockade of non-specific bindings by incubating the membranes, overnight, in 5% low-fat milk in 1x TBS. After this incubation, the membranes were washed 2x5min with 100mL of TBS-T.

Then, the membranes were incubated with primary antibody, α-PBEF (rabbit, Santa Cruz Biotechnology), diluted 1:1000 in a solution with 1% low-fat milk in 1% TBS-T, for 2 hours at room temperature, followed by a new wash, 3x20min, with 1% low-fat milk in TBS-T.

A secondary antibody, goat anti-rabbit IgG (Santa Cruz Biotechnology), diluted 1:5000 was then added to bind the primary antibody and incubated for 1 hour at room temperature, diluted in the same solution as the primary – 1% low-fat milk in 1% TBS-T. After this last incubation, the membranes were again washed 3x10 min with 1x TBS-T.

Detection was performed by chemiluminescence, using the Amersham Hybond-ECL kit. The detection mixture was left for 1min at room temperature, and the excess was drained off the membrane. The membrane was isolated inside a transparent film and placed in an X-ray film cassette for different exposure times and then developed with developer and fixer solutions (SIGMA).

Structural Analysis

The NAMPT-like protein model was obtained by homology modelling using MODELLER [55] with the human NAMPT structure as a template, retrieved from PDB

(http://www.rcsb.org/pdb/home/home.do). Structures were aligned and visualize in PyMOL [56], an open-source tool to visualize molecules.

Geneious

Geneious (version 5.5.7) is a software that combines a wide variety of sequence analysis tools and was used to compare sequences obtained with reference ones, to detect polymorphisms. [54].

Important Sites

During the research for this thesis several important sites and scientific databases were used, such as: Protein Data Bank (PDB - http://www.rcsb.org/pdb/home/home.do), National Center for Biotechnology Information (NCBI - http://www.ncbi.nlm.nih.gov/), EnsEMBL Genome Browser (EnsEMBL - http://www.EnsEMBL.org/index.html), Catalogue of Somatic Mutations in Cancer (COSMIC - http://www.sanger.ac.uk/perl/genetics/CGP/cosmic), PubMed (US National Library of Medicine National Institutes of Health - http://www.ncbi.nlm.nih.gov/pubmed), The Human Protein Atlas (http://www.proteinatlas.org/), Multalin (http://multalin.toulouse.inra.fr/multalin/), Modeller (http://salilab.org/modeller/) [55], ProSa-web (https://prosa.services.came.sbg.ac.at/prosa.php) [57-58], Polyphen (http://genetics.bwh.harvard.edu/pph2/) [59], and OligoCalc (http://www.basic.northwestern.edu/biotools/oligocalc.html).

RESULTS

DNA Analysis

In order to study the DNA polymorphisms from both NAMPT and NAPRT genes in human tumor cells, PCR reactions were performed as described in Materials and Methods. The target regions were chosen according to the polymorphisms already described in the NCBI SNP and EnsEMBL databases: exons 2, 4, 7, 8 and 9 and intron 4 for NAMPT, and exons 2 and 7 for NAPRT.

NAMPT polymorphisms

The results obtained for PCR amplification of the NAMPT gene are shown in the next figures (figure 5-9). As we can see NAMPT gene was amplified, with the conditions presented in Materials and Methods, in all samples tested.

Results

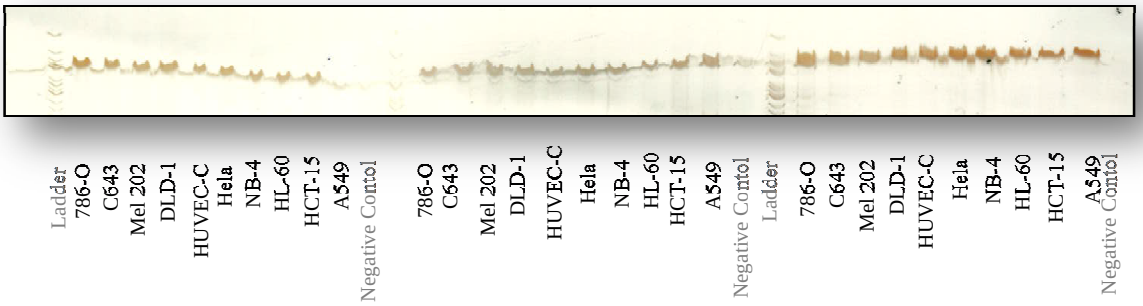

Figure 5 – Acrylamide gel with NAMPT amplicons obtained with primers for exons 2,7 and 9

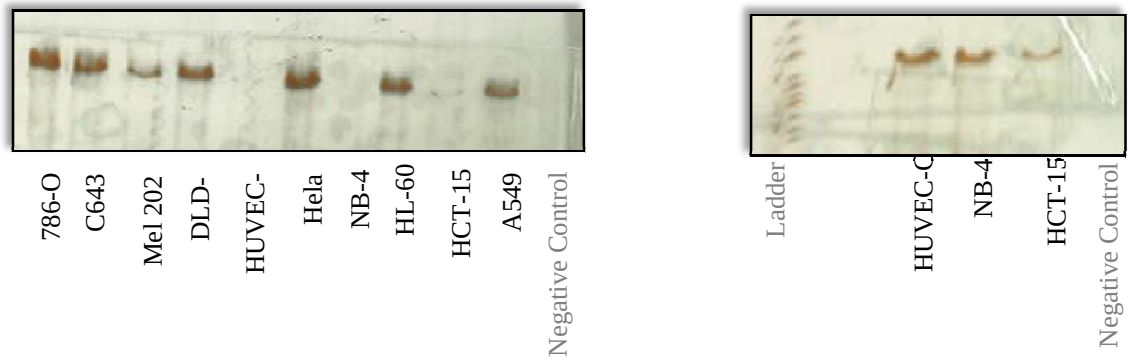

Figure 6 – Acrylamide gel with NAMPT amplicons obtained with primers to exon 4. The image on the right is the repetition of the PCR for three samples that had failed to amplificate, previously.

Figure 7 - Acrylamide gel with samples amplified with primers to intron 4.

Results

Figure 8 - Acrylamide gel with samples amplified with primer to exon 4 (forward) and intron 4 (reverse) to amplify the region between the beginning of exon 4 and the end of intron 4. Samples Mel202 and A549 were repeated separately.

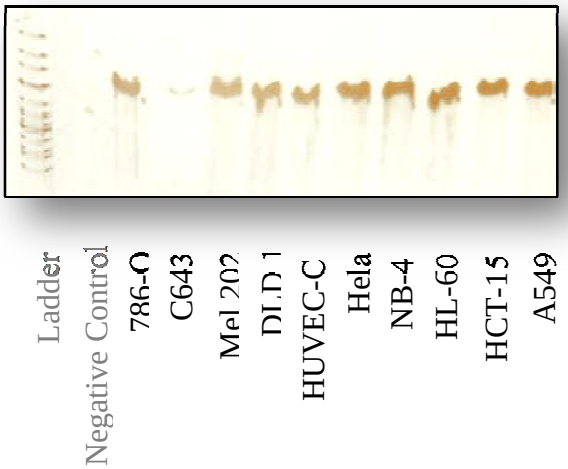

Figure 9 - Acrylamide gel with samples amplified with primers to exon 8. C643 shows a very weak band and was repeated separately.

With the aim to search for polymorphisms all the samples were sequenced (Materials and Methods) and analyzed with Geneious software, by comparing the sequences of the cell lines with the reference sequence obtained in NCBI (NAMPT GeneID 1035). A polymorphism in exon 7 of the NAMPT gene was found in cell lines C643, Mel 202, HUVEC-C, Hela, NB-4, HL-60 and A549. This polymorphism was already described in dbSNP, as rs11553095 and corresponds to a synonymous substitution as described in table 6. Moreover, two intronic polymorphisms were found in intron 4, already described in dbSNP, as rs28454100 and rs34056375. A novel polymorphism was found in exon 8 in A549 sample, as described in table 6.

Although lacking confirmation with the reverse primer, the polymorphism in position 13195 was detected with different pairs of primers and with independent PCR protocols (figure 10). Comparison with the reference sequence that has a T in position 13195 shows that Hela has a G in the same position.

Results

Table 6 – Information about the polymorphisms found in NAMPT gene. The information was collected in NCBI and EnsEMBL.

Gene	Exon/ Intron	DNA Pos.	mRNA Pos.	Alelle Change	AA Pos.	AA change/ Type	ID	Found in
NAMPT	Intron 4	13195	/	TTT> TTG	/	/	rs28454100	Hela
NAMPT	Intron 4	13422	/	GGT> AGT	/	/	rs34056375	C643, HUVEC-C, HL-60, A549
NAMPT	Exon 7	23469	1211	TCA> TCG	301	Ser -> Ser Synonymous	rs11553095	C643, Mel 202, HUVEC-C, Hela, NB-4, HL-60, A549
NAMPT	Exon 8	23531	1323	AAG> GAG	339	Lys->Glu non-synonymous	/	A549

Results

Rs28454100

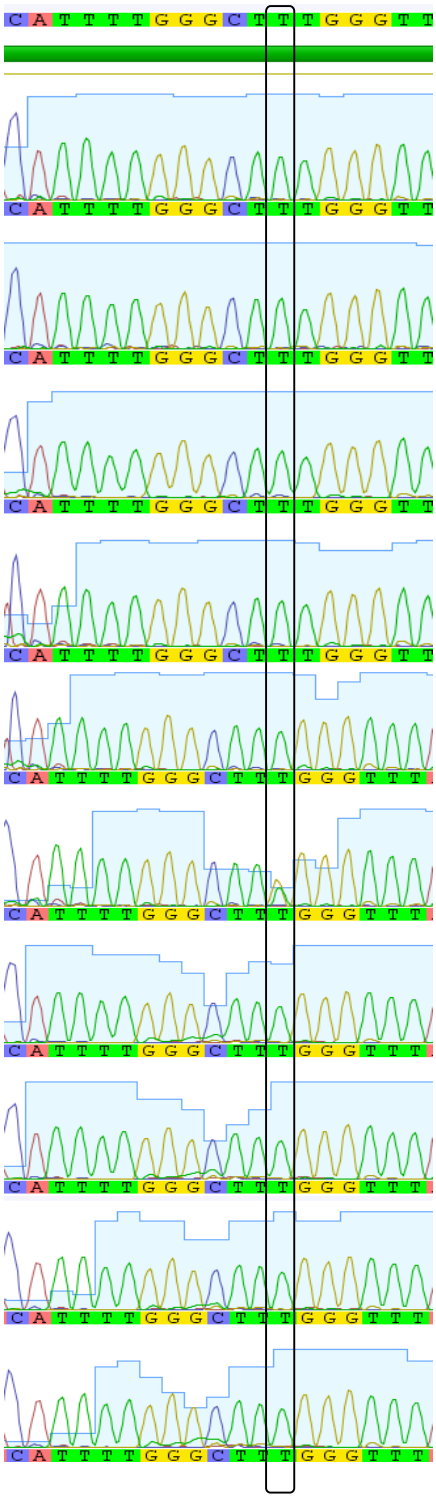

Figure 10 – rs28454100. Alignment of the ten cell lines sequences showing the rs28454100 polymorphism found in NAMPT gene, in Hela sample

Results

Rs34056375

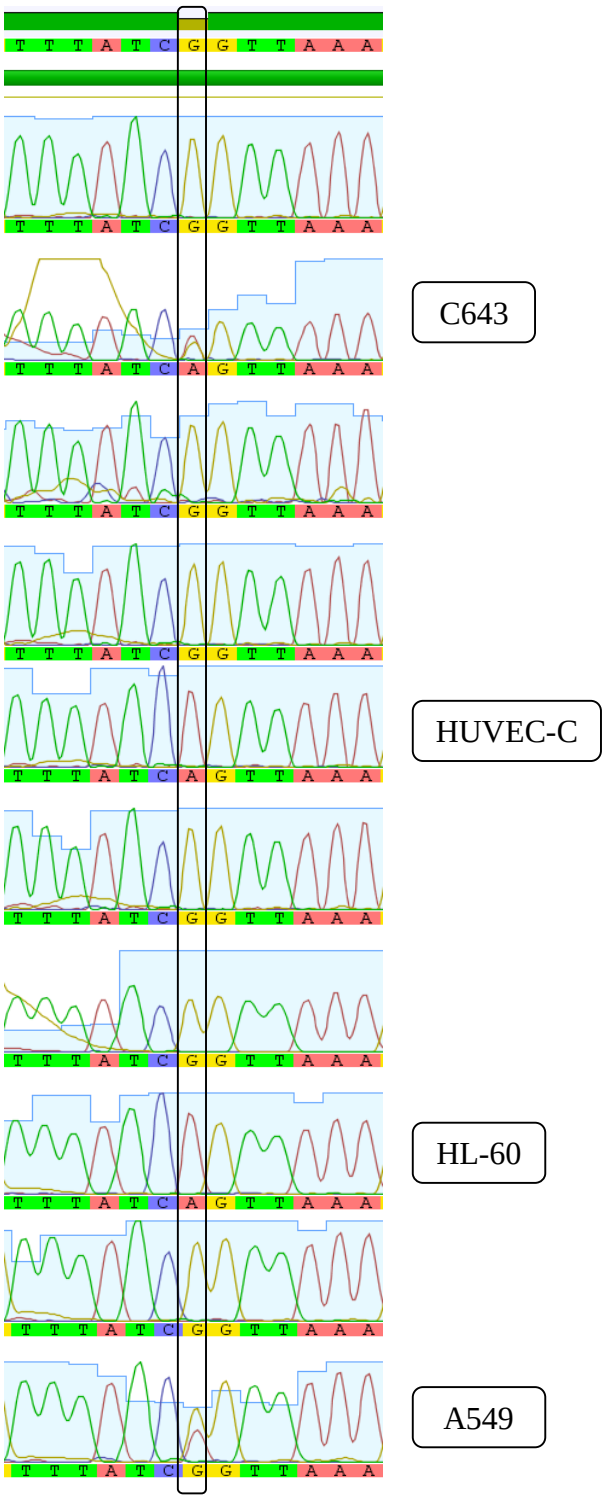

Figure 11 - rs34056375. Alignment of the ten cell lines sequences showing the rs34056375 polymorphism found in NAMPT gene, in C643, HUVEC-C, HL-60 and A549

Results

Comparison with the reference sequence that has a G in position 13422 shows that some samples have an A in the same position (HUVEC-C and HL-60), and others (C643 and A549) show a heterozygotic pattern (figure 11).

Rs11553095

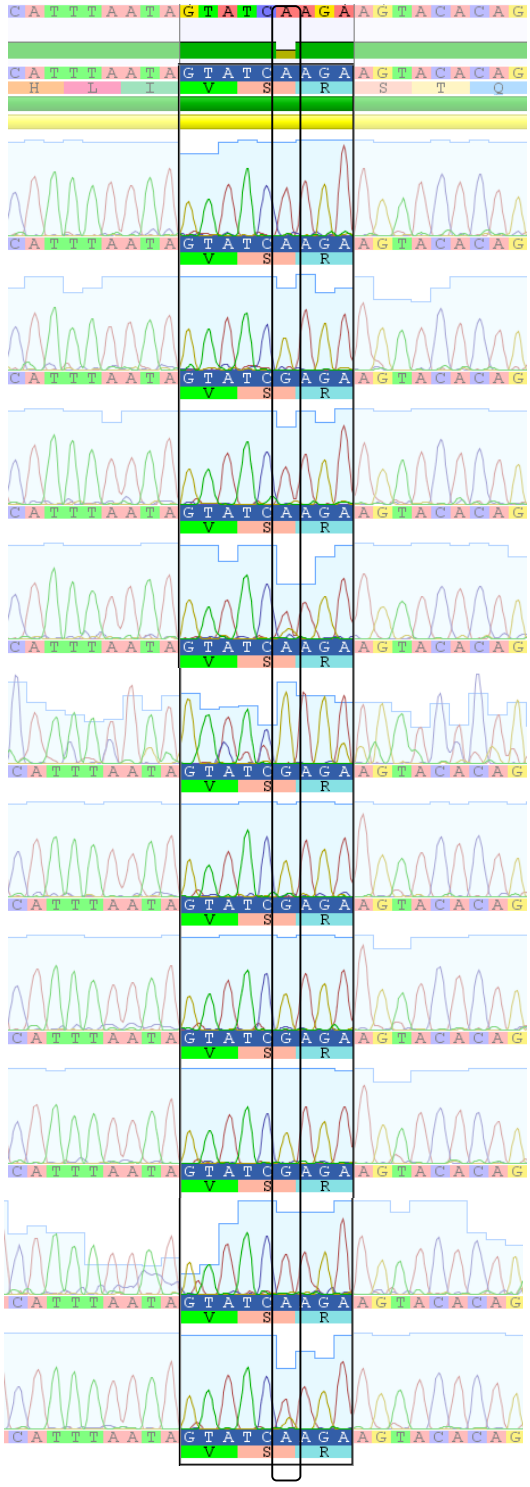

Results

Figure 12 - Rs11553095. Alignment of the ten cell lines sequences showing the rs11553095 polymorphism found in NAMPT gene, in C643, MEL 202, HUVEC-C, Hela, NB-4, HL-60 and A549

Comparison with the reference sequence that has an A in position 23469 shows that some samples have a G in the same position (C643, HUVEC-C, Hela, NB-4 and HL-60), and others (Mel 202 and A549) show a heterozygotic pattern (figure 12).

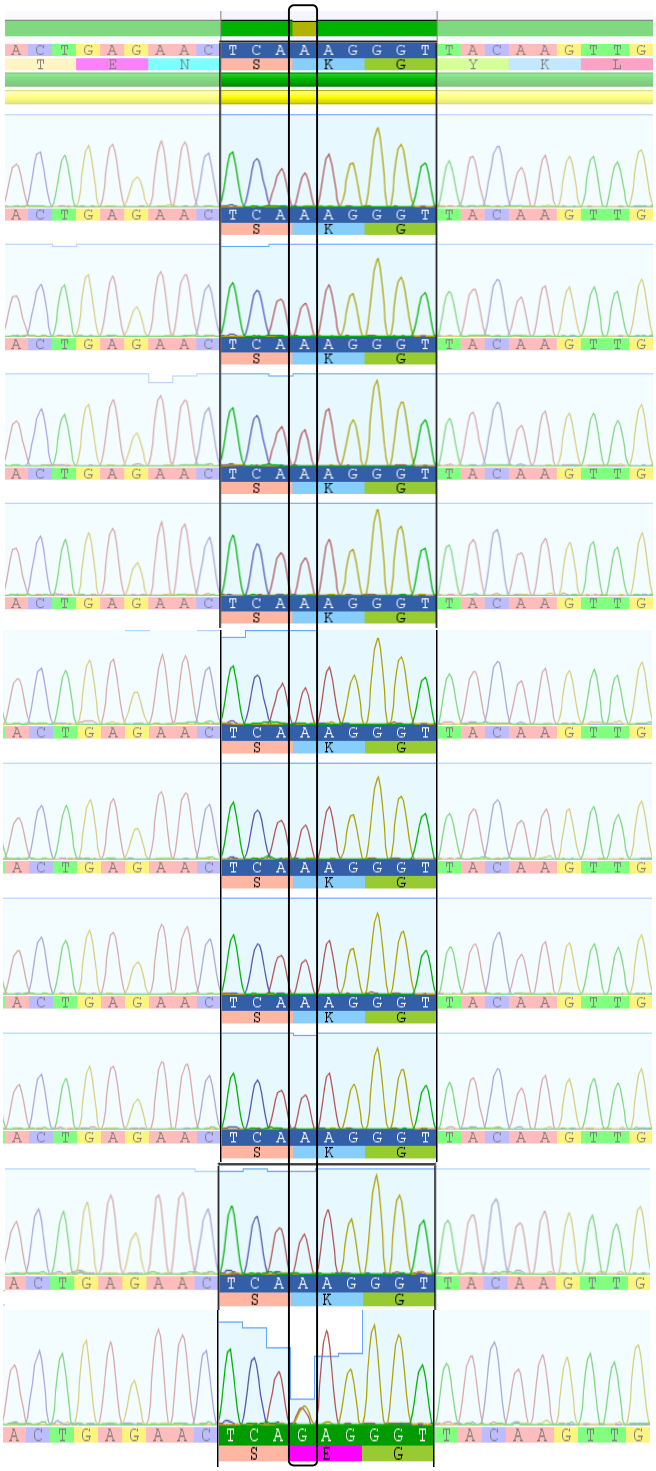

A549

Results

Figure 13 – Novel polymorphism. Alignment of the ten cell lines sequences showing the novel polymorphism found in NAMPT gene, in A549 sample

The polymorphism found in exon 8 was a novel one and it is presented in the previous figure (figure 13).

In order to study the consequences of this novel polymorphism the website Polyphen was used, and this modification is predicted to be benign.

The concatenation of all the sequences obtained for all the samples was carried out with Geneious software (figure 14).

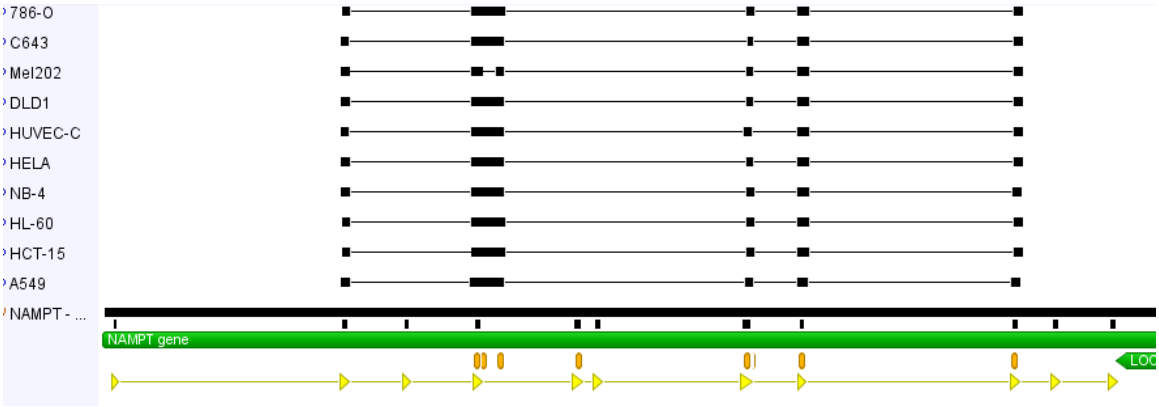

Figure 14 – NAMPT gene sequences obtained for all the samples tested. The sequence between the region amplified with primers to exon 4 and the region amplified with primers to intron 4 was not obtained for Mel 202 sample.

NAPRT polymorphisms

A similar approach was performed for NAPRT gene with differences described in Materials and Methods. The images obtained are shown below.

Exon 2 Exon 7

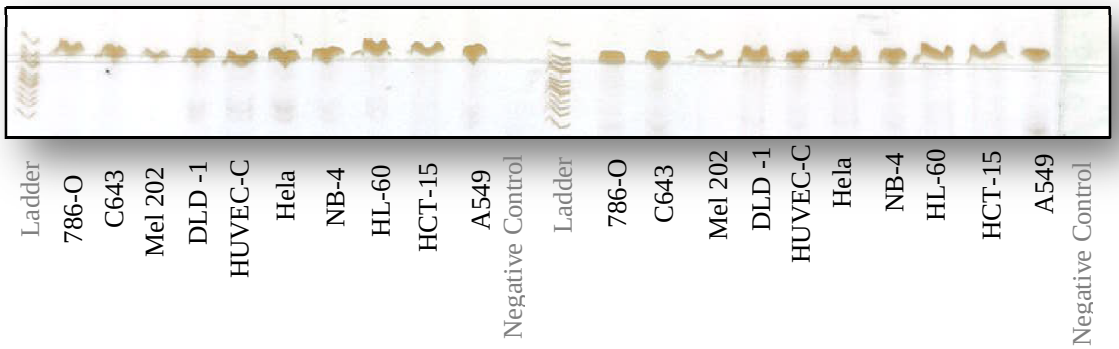

Results

Figure 15 – Acrylamide gel with fragments amplified with primers for NAPRT exons 2 and 7

Samples were sequenced and compared to the reference sequence obtained in NCBI (NAPRT GeneID 93100). In the NAPRT gene, two polymorphisms were found, one in exon 2 and one in exon 7 (table 7). Both these polymorphisms are already described in databases as rs896954 and rs872935, respectively, and result in synonymous amino acid substitutions. Rs896954 was found in C643, HUVEC-C and HL-60 cell lines, while rs872935 was found in all cell lines tested but HL-60.

Table 7 - Information about the polymorphisms found in NAPRT gene. The information was collected in NCBI and EnsEMBL.

Gene	Exon/ Intron	DNA Pos	mRNA Pos	Alelle Change	AA Pos	AA change Type	ID	Found in
NAPRT	exon 2	1374	319	GCC >GCT	98	Ala->Ala Synonymous	rs896954	C643, HUVEC-C, HL-60
NAPRT	Exon 7	2709	934	CTG >TTG	305	Leu->Leu Synonymous	rs872935	All but HL-60

Results

rs896954

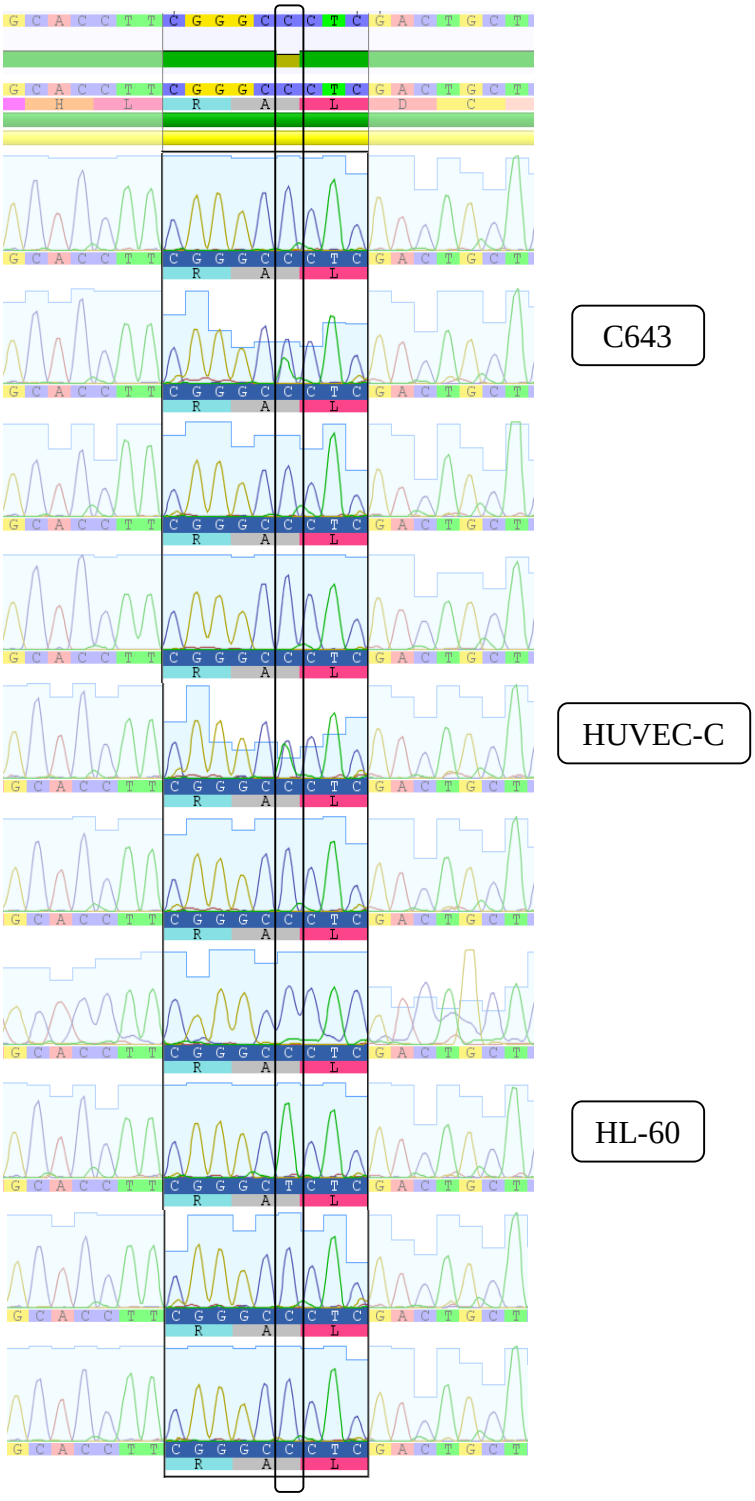

Figure 16 – rs896954. Alignment of the ten cell lines sequences showing the rs896954 polymorphism found in NAPRT gene, in C643, HUVEC-C and HL-60

Results

For rs896954, the reference sequence has a C and samples show a T in a homozygotic (HL-60) or heterozygotic (C643 and HUVEC-C) pattern (figures 16).

rs872935

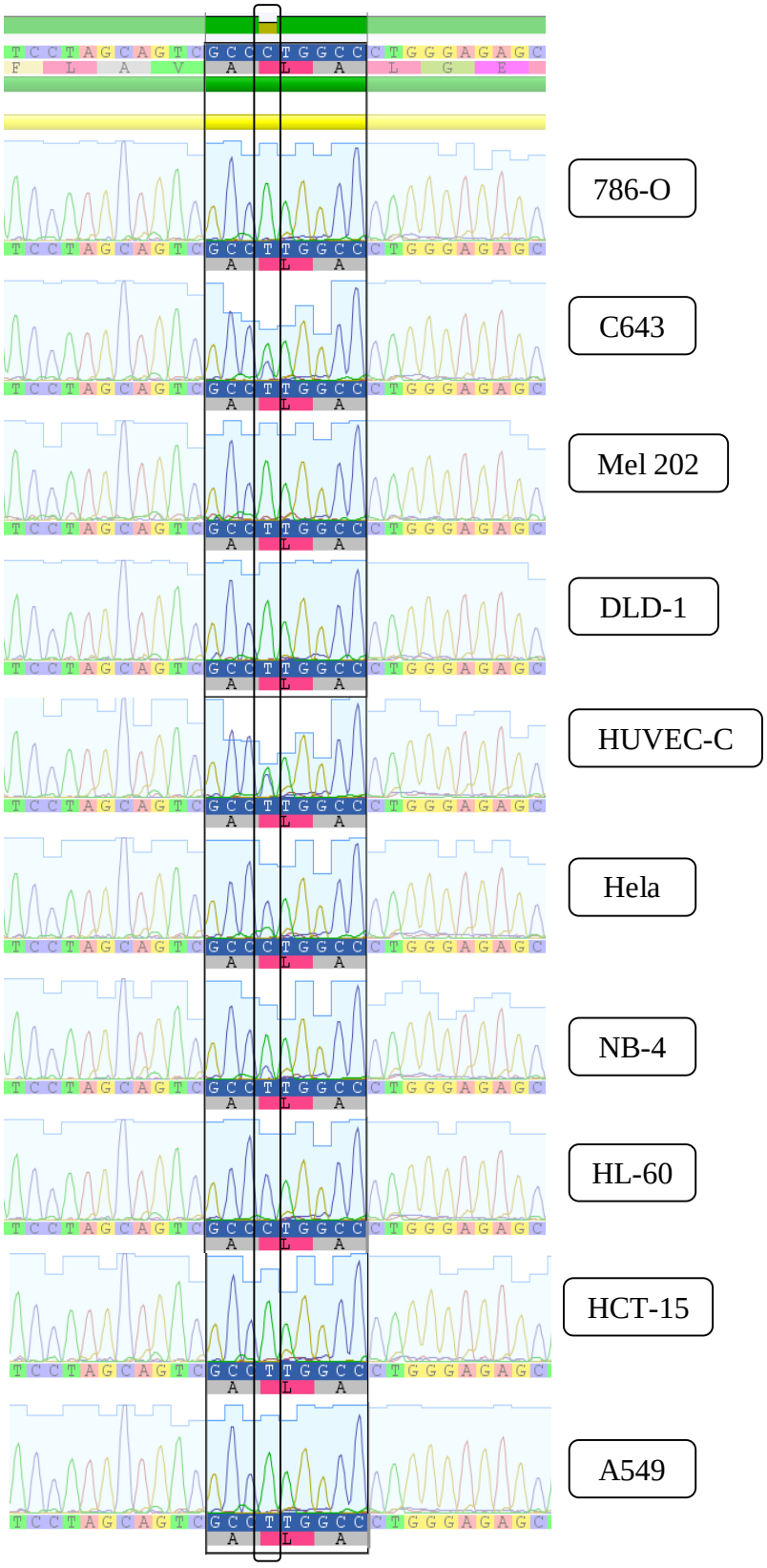

Results

Figure 17 - rs872935. Alignment of the ten cell lines sequences showing the rs872935 polymorphism found in NAPRT gene, in all samples but HL-60

For the polymorphism rs872935, cell lines A549, HCT-15, Mel-202, DLD-1 and 786-O are homozygotic, while samples Hela, HUVEC-C, NB-4 and C643 show the same polymorphism in a heterozygotic pattern (figure 17).

The sequences obtained for the NAPRT gene were align and concatenated as previously (figure 18).

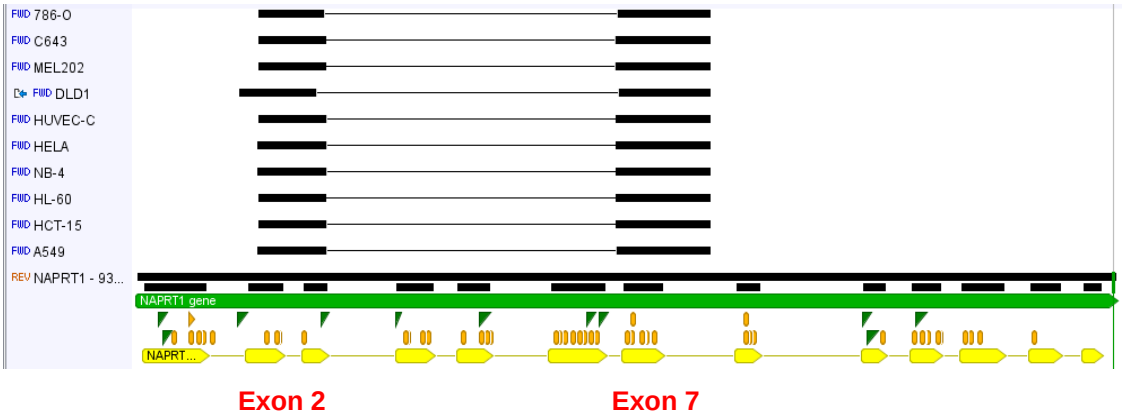

Figure 18 – NAPRT gene sequences obtained for all the samples tested. The image was obtained with software Geneious.

RNA Analysis

To study NAMPT and NAPRT expression in human tumor cell lines, RT-PCR was used to amplify the fragments of interest (using primers and programs already described in section Materials and Methods). The amplification was confirmed with acrylamide gels (figure 19). Fragments were sequenced and the analysis was performed in Geneious, comparing sequences with the reference ones (NAMPT 1035-NAMPT mRNA and NAPRT 93100-NAPRT mRNA).

For NAMPT, due to the possible expression of the pseudo-gene, NAMPT-like that differs from NAMPT by the lack of exon 1 and several SNPs (figure 32) four pairs of primers were used to amplify the entire coding sequence. For NAPRT, the region amplified corresponds to the exons 9-13 where transcript differences are predicted to

Results

occur. The sample DLD-1 failed in most amplifications and was excluded from further analysis.

An additional agarose gel was performed in order to detect qualitative expression differences between the cell lines, including GAPDH amplification as a control (figure 20)

NAMPT expression

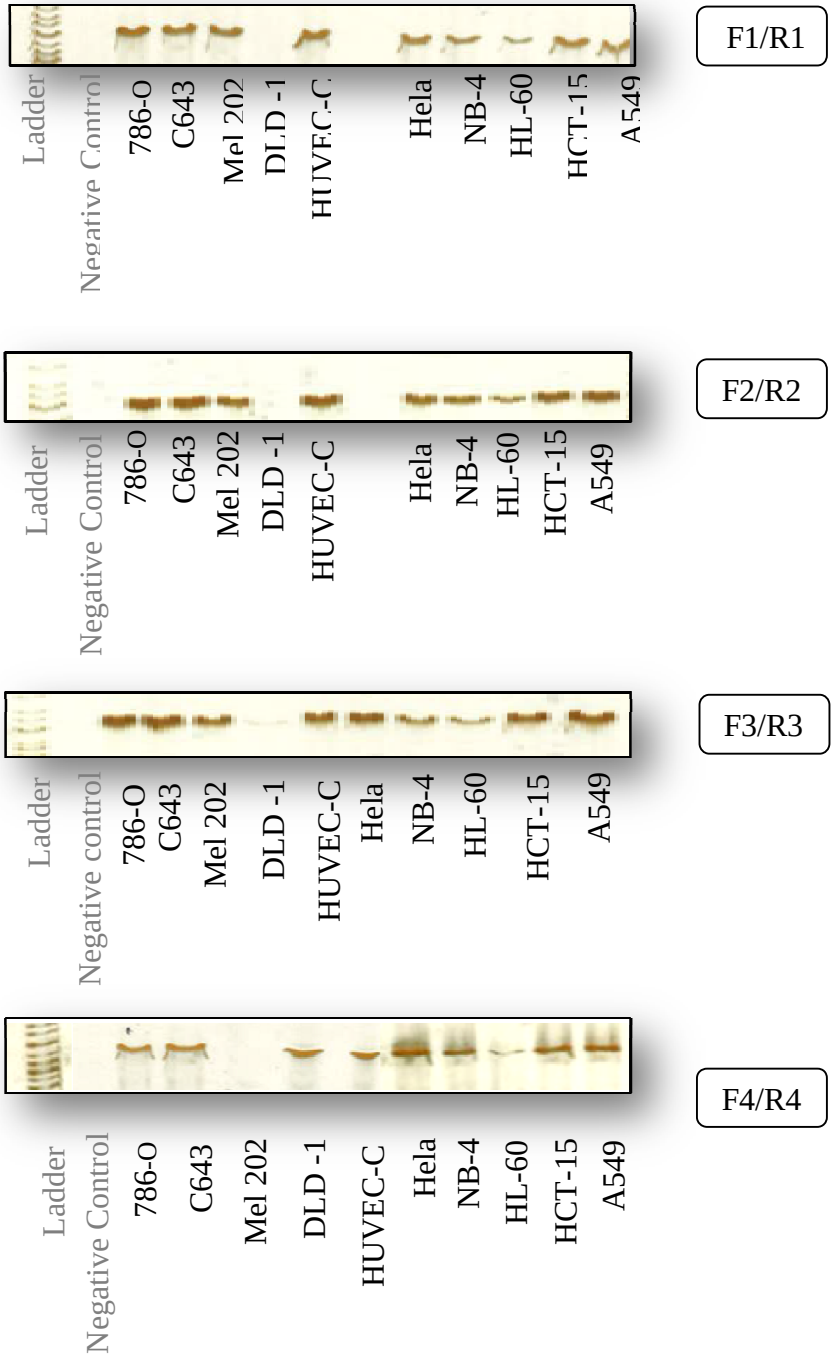

Results

Figure 19 - Acrylamide gel with the ten samples studied and amplified with primers for NAMPT transcript. Mel 202 has failed to amplify fragment F4/R4 and was repeated separately.

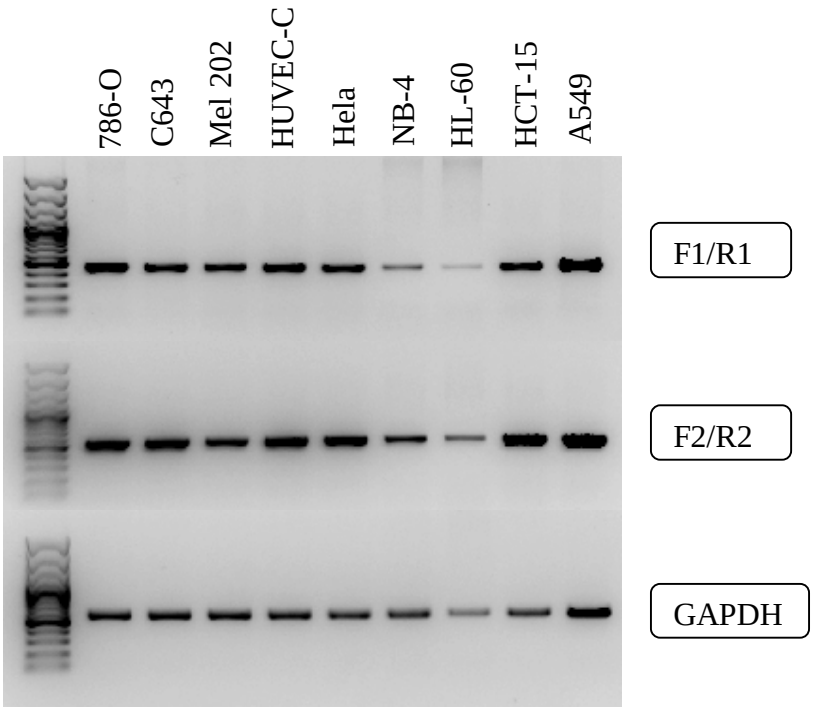

Figure 20 – Agarose gel with NAMPT expression in all the samples tested, except DLD-1. GAPDH was used as a control.

Products amplified with F1/R1 (NAMPT-only) and F2/R2 (NAMPT and NAMPT-like) were run on agarose gels (figure 20). Presumed expression of NAMPT-like was not observed, however there are apparent expression differences between the samples. To confirm if NAMPT-like was actually expressed, the analysis of the sequences focused in the differences presented in table 8 and figure 21. A more detailed description of the differences tested is described in Appendix.

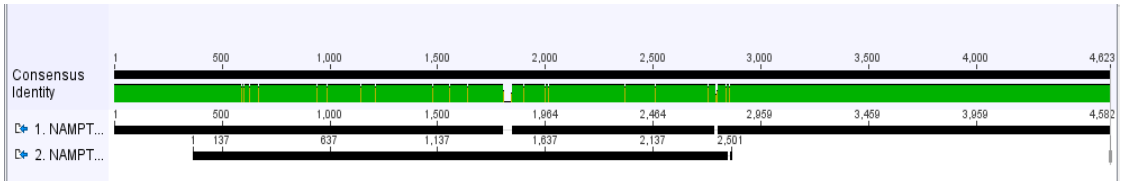

Figure 21 – Representation of the alignment of NAMPT and NAMPT-like obtained with software Geneious

Results

Table 8 - Representation of the nucleotide differences between NAMPT and NAMPT-like with each pair of primers used. The sequencing analysis was focused in the search for these differences.

Primers	NAMPT	NAMPT-like
F1/R1	✓	NO
F2/R2	594T	594G
	605G	605A
	629G	629A
	671G	671A
	941C	941T
	988T	988A
F3/R3	1143G	1143A
	1211A	1211G
F4/R4	1478G	1478A
	1559A	1559G
	1640G	1640A
	1813A	1813G

The alignments do not show evidence that NAMPT-like was expressed, however the fragment F3/R3 was misleading due to the polymorphism present in the samples that was already described in NAMPT DNA (exon 7 – rs11553095).

The complete transcript sequences were concatenated with software Geneious, and the resulting images are presented in Appendix.

NAPRT expression

For NAPRT cDNA, the study was performed with primers GSP2/R2 Hara that amplify the coding sequence from exon 9 until the end and the resulting gel is shown below (figure 22).

Results

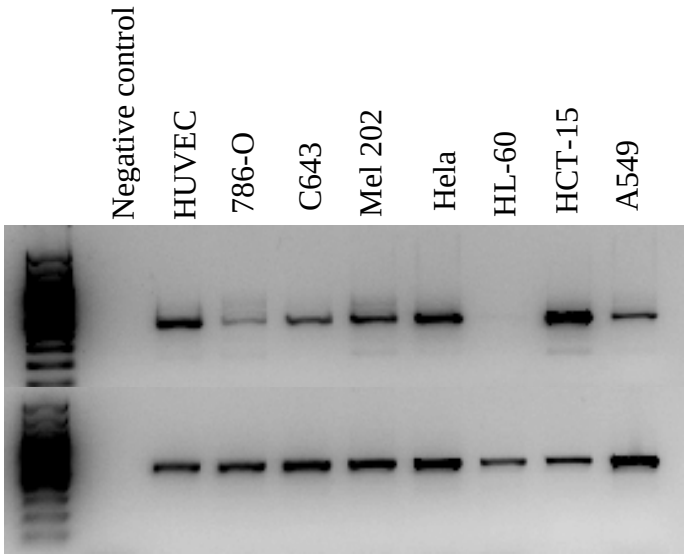

Figure 22 - Agarose gel showing expression of NAPRT samples amplified with primer GSP2/R2 Hara (top panel). GAPDH expression was included as control (down panel).

It is shown that NAPRT is expressed in all samples represented, albeit at different levels. 786-O and HL-60 express less NAPRT and an additional band is present in Mel 202 and HCT-15 that is predict to be an alternative NAPRT transcript.

Protein Analysis

NAMPT protein expression was further studied, through a Western-Blot technique (figure 23).

Western-Blot

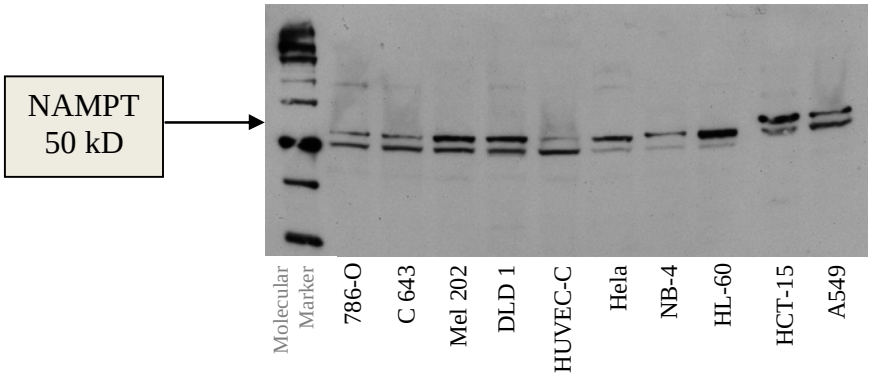

Figure 23 – Western-Blot with antibodies against NAMPT protein.

The image shows that all human tumor cell lines express the protein, confirming the results obtained at the RNA level. However, there are two bands around 50kD with

a different pattern of expression between the samples that could represent different NAMPT isoforms.

Structural Analysis

In order to infer about the structural and functional consequences of NAMPT-like mutations, a protein model was studied in PyMol. An alignment of NAMPT (3DKJ, obtained in PDB) and NAMPT-like was used in MODELLER [55] to build a 3D structural model (figure 24). Three amino acid substitutions were evaluated, the phenilalanine (F) in position 96 of NAMPT protein that is substituted by a valine (V) in the correspondent position (65) of the NAMPT-like protein; isoleucine (I) in position 227 that is replaced by asparagine (N) in the correspondent position (196) of NAMPT-like; the substitution of aspartic acid (D) in position 279 by asparagine (N) in the correspondent position (248) of the NAMPT-like protein.

Figure 24 – Overall alignment of NAMPT (PDB code 3DKJ, in green) with the NAMPT-like model (blue). Images were obtained in Pymol.

Results

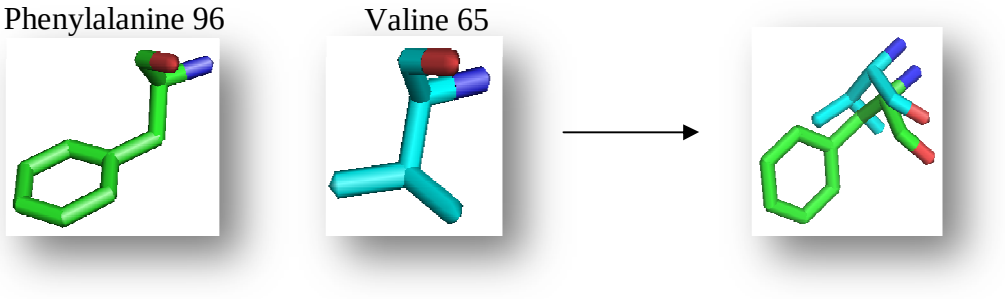

Figure 25 - Representation of phenylalanine 96 of NAMPT protein and the corresponding valine 65 of NAMPT-like protein. The figure on the right represents the alignment of these two aminoacids.

The first amino acid modification considered is the substitution, in position 96 of NAMPT protein, of a phenylalanine (F) by a valine (V) in position 65 in NAMPT-like protein (figure 25 and 26). The loss of a polar contact with a water molecule (position 620 in NAMPT) can be detected in the NAMPT-like protein. The interaction with E98 (NAMPT) and the corresponding E67 (NAMPT-like) is maintained, although there is a slight conformational change due to the shorter size of the amino acid.

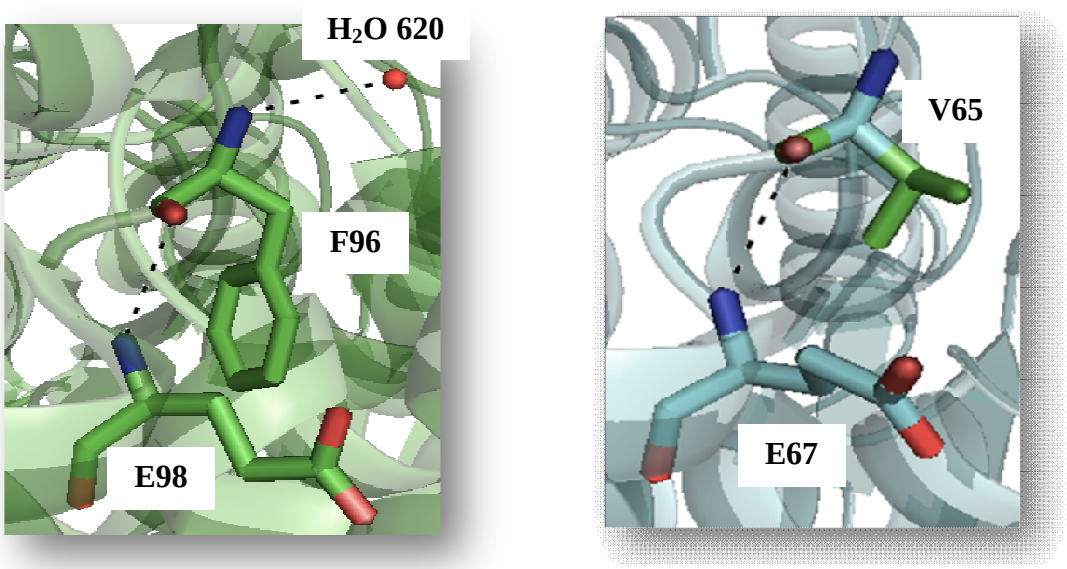

Figure 26 – F96V substitution. NAMPT is represented in the left and NAMPT-like in the right. NAMPT-like loses a polar contact with a water molecule located in position 620 of NAMPT.

The second modification involves isoleucine (I) 227 and asparagine (N) 196. Both amino acids are represented in the following image (figure 27).

Results

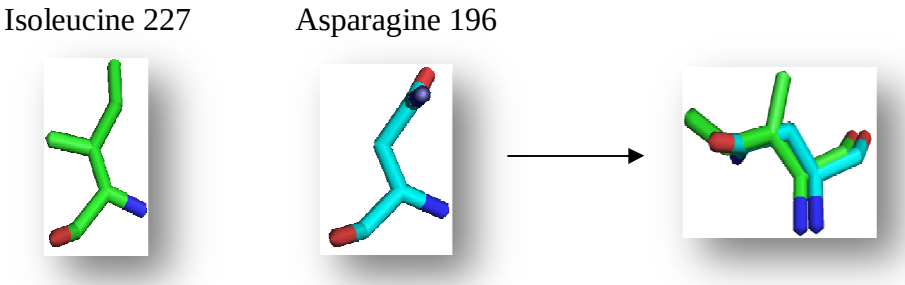

Figure 27 - Representation of isoleucine 227 of NAMPT protein and asparagine 196 of NAMPT-like protein. The figure on the right represents the alignment of these two aminoacids.

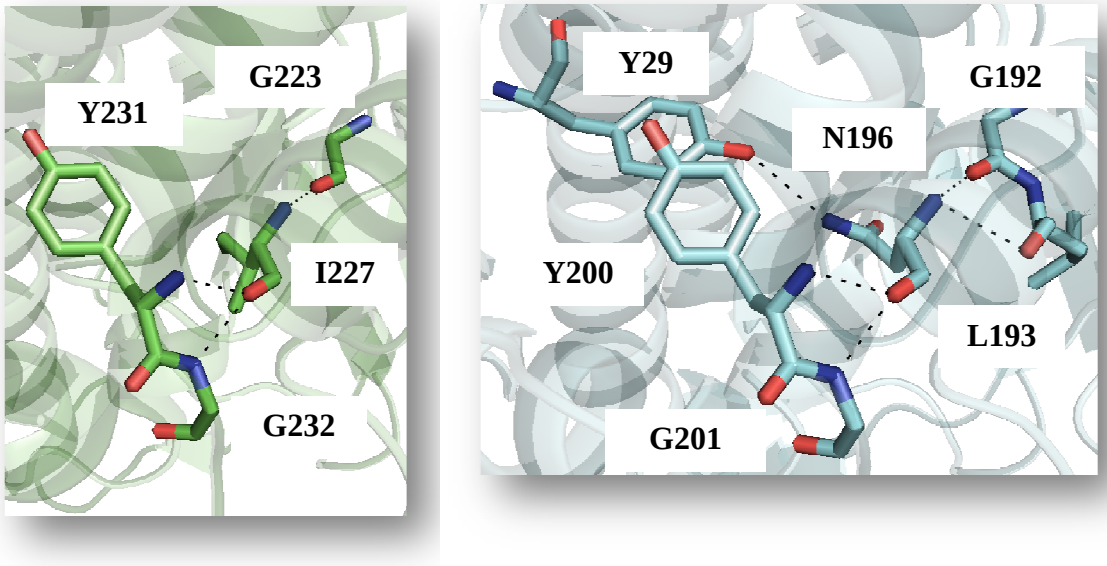

Figure 28 – I227N substitution. NAMPT is represented in the left and NAMPT-like in the right. NAMPT-like establishes new polar contact with Y29 and L193, being all the other connections the correspondent ones in NAMPT.

In figure 28, I227 connections in NAMPT are compared to N196 connections in NAMPT-like and it shows that NAMPT-like establishes new polar contacts with Y29 and L193, being all the other connections the correspondent ones in NAMPT.

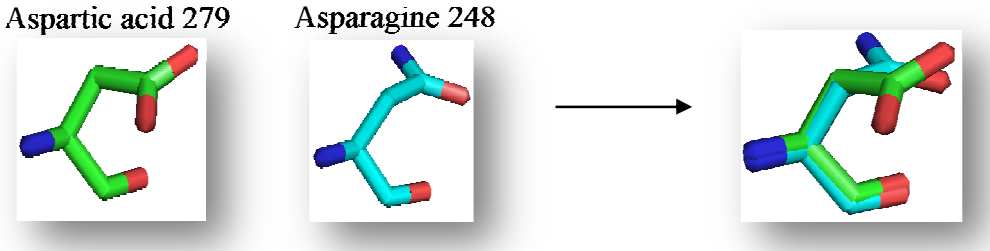

Figure 29 - Representation aspartic acid 279 of NAMPT protein and asparagine 248 of NAMPT-like protein. The figure on the right represents the alignment of these two aminoacids.

Results

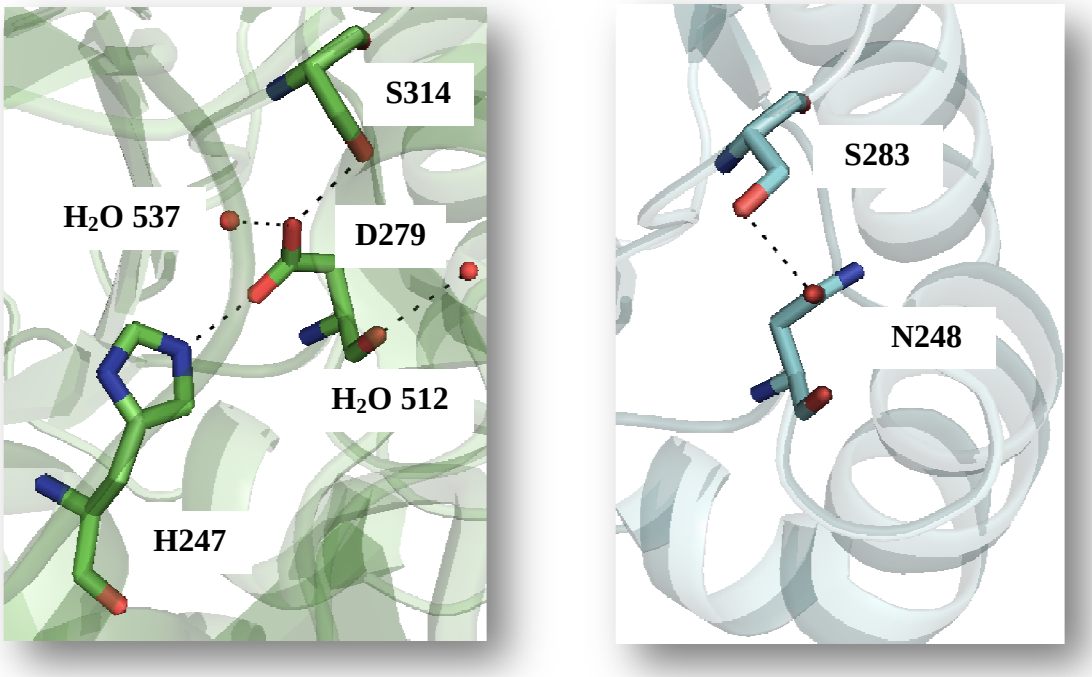

Figure 30 – D279N substitution. NAMPT is represented in the left and NAMPT-like in the right. NAMPT-like loses a polar contact with H247 and H_2O 512 and 537 (of the second chain)

Figure 30 show that NAMPT-like loses polar contacts with H247 and H_2O 512 and 537.

The next table outlines the consequences of the missense mutations analyzed with the NAMPT-like protein model and shown in the above images. All three modifications are predicted to be damaging, being the third modification the most important one because of its structural and functional effect.

Results

Table 9 - Review of the consequences of the three amino acid modifications of the NAMPT-like protein

NAMPT nt	NAMPT-like nt	aa	Prediction (Polyphen)	PyMol	Substituition effect (Polyphen)
TTT	GTT	F96V	PROBABLY DAMAGING	Loss of a polar contact with a molecule of water (H_2O 620)	/
ATT	AAT	I227N	PROBABLY DAMAGING	New connection with Y29 e L193	structural effect, buried site, Hydrophobicity change at buried site
GAT	AAT	D279 N	PROBABLY DAMAGING	Loss of three polar contacts (H247 and H_2O 512 e 537)	functional effect, indirect Contact with functional site

DISCUSSION

Cancer cells have increased NAD requirements and due to this fact inhibitors of NAMPT are currently in clinical trials as novel cancer therapeutics agents. However these drugs show some citotoxicity that can be overcome by adding NA that will activate NAPRT as an alternative NAD synthesis pathway. NAPRT is absent in some tumors, like neuroblastoma, glioblastoma [60] and lymphoma [44]. Although being a promising field there is a lack of information about NAPRT expression in literature and databases and a few experimental studies concerning expression of this gene were made in mouse and rat [38]. This is a limiting factor to infer about the use of NAPRT as a biomarker for the use of nicotinic acid as a chemoprotectant in treatment with NAMPT inhibitors.

So, in the present work the expression of the two main genes in NAD salvage pathway was studied showing that both NAMPT and NAPRT are expressed in all human tumor cell lines tested. In fact, this information predicts that although some

Discussion

cancers are NAPRT negative, others actually express this gene, making these novel therapeutic not suitable to all cancers.

In addition, polymorphisms found in the DNA may explain different expression levels of these genes or the presence of novel isoforms in some tissues. Mutations can be in exons, splice site regions, intronic regions or in untranslated regions.

Splice site polymorphisms can lead to errors during the processing of pre-mRNA into mature messenger RNA, by inserting or deleting nucleotides in the specific site at which removal of the intron takes place [61].

It is well known that problems in mRNA splicing are an important bridge to disease. About 90% of exons are interspersed by intronic dinucleotides GT and AG at the 5' and 3' splice sites respectively, so mutations in these regions can lead to elimination of the adjacent exon [61].

Modifications in the splicing pattern can cause truncation of the enconded protein, an in frame insertion or deletion of structural and functional domains or the substitution of N and C-termini. Modifications of this kind can change proteins in structure, function and interactions, which can lead to a disease condition. [61-62].

More specifically in tumorigenesis, changes in splice sites are described to have a crucial role, either by inactivating tumor suppressor genes or by gain of function of proteins promoting tumor development [62].

NMD, nonsense mediated decay, is a cellular mechanism of RNA degradation involved in the detection of nonsense mutations in order to avoid the expression of truncated or damaged proteins. It is a process that degrade erroneous transcripts that contain premature termination codons (PTC) being responsible for dynamically altering gene expression [63].

Concerning tumorigenesis, NMD was shown to degrade transcripts involved in the adaptative response of cells to their microenvironment. Moreover and due to the existence of PTC in many suppressor genes mutated in cancer, NMD is already accepted as a preventing factor of tumorigenesis [63].

Another region where polymorphisms can occur is three prime untranslated region – 3 prime UTR – a particular section of messenger RNA that follows, immediately, the stop codon of the coding region [64].

The regulation of protein synthesis occurs by both cis-regulatory elements (DNA sequences next to the structural portion of a gene required for gene expression) located

in the 5' and 3' UTR and trans-acting factors (factors that bind to the cis-regulatory sequences in order to control gene expression [64].

The 3' UTR is a very important region due to its roles in translation, localization and stability of the mRNA. So, mutations in the termination codon, polyadenylation signal and secondary structure of this region can lead to disease [64].

Specifically in NAMPT and NAPRT genes, several synonymous polymorphisms were detected and a novel missense mutation, not yet described in databases, was found in the human tumor cell lines studied. Although the target regions were selected to include the main polymorphisms known, the discovery of a previously uncharacterized polymorphism suggests that the genetic screen should be performed across the entire length of the gene for a complete characterization and to uncover potential novel mutations.

Synonymous mutations are also known as "silent" mutations, but are currently described to cause changes in protein expression, conformation and function. Several studies link these types of mutations to human disease risk and treatment outcomes despite that until now the main focus has been given to mutations that are able to change the amino acid sequence of a protein –non-synonymous or missense mutations [65].

Due to the intrinsic idea that the structure and function of a protein is dictated by the amino acid sequence and owing to the property of degeneracy of the genetic code, synonymous mutations do not alter the amino acid sequence and, therefore, were referred to as silent [65]. Until now. Several important studies are revealing that synonymous mutations can actually affect mRNA stability and modify protein expression, culminating in human diseases [65].

In the polymorphism found in exon7 of NAMPT gene (rs11553095), allele G is 71.8% prevalent comparing to allele A, according to dbSNP for the normal population. Regarding the homo and heterozygotic pattern, A/A has a percentage of 7.7%, A/G 41% and G/G 51.3%. The results of the samples tested are similar to the results for the normal population, being the pattern G/G the most found.

Regarding the polymorphim in intron 4 of NAMPT gene (rs28454100), G is prevalent in 96.7% of the normal population. This information is consistent with the

Discussion

results for the tumor samples that show G and T (heterozygotic pattern) only in Hela samples, whereas all the other samples present G in a homozygotic pattern.

For the second polymorphism in intron 4 of the same gene (Rs34056375), G is 72.5% prevalent comparing to allele A. The results of the tested samples follow the trend of the normal population, being the pattern G/G the most found.

The polymorphism in exon 2 of NAPRT gene (rs896954) shows a notable incidence of the C (reference sequence) versus the T allele, in the normal population (95.8% vs 4.2%). This pattern is similar in the human tumor samples tested.

In the polymorphism found in exon 7 of NAPRT gene (rs872935), the human tumor samples show decreased occurrence of the C allele comparing to T. For example, the CC pattern is present in about 30% of the normal population but was not observed in the human tumor samples.

Considering the expression of NAMPT and NAPRT, there are qualitative differences between tumor cell lines in both genes, however due to the fact that PCR protocol is not quantitative, a reliable conclusion about the difference patterns depends on a real-time PCR protocol.

NAMPT was shown to be expressed in all cell lines tested, whereas the presence of NAMPT-like was not proved although there is a visual difference in the expression pattern between F1/R1 and F2/R2 fragments. Curiously, both leukemia HL-60 and NB-4 samples show a decreased expression pattern for NAMPT cDNA. NAPRT is expressed in all cell lines tested, however, 786-O and HL-60 samples shown a decreased NAPRT expression. Another finding shown is the presence of a smaller transcript in all samples, with different expression patterns, where the samples showing a stronger band are Mel 202 and HCT-15.

DLD-1 was not integrated in the expression studies due to its repeated failures in amplification and since HCT-15 is also a colorectal cancer cell line, it is expected that similar results would be obtained from both. However, comparison of different cell lines from the same tissue should be carried out in order to validate the results.

The new NAPRT transcript must be better studied, as it is important to determine which transcript is expressed in which tissue and if there are significant differences between normal and tumoral tissues. An open question is the expression of

Discussion

NAMPT-like that was not detected in the cell lines used. These questions are being addressed.

Regarding the protein analysis, an additional NAMPT isoform was detected by Western-Blot. The significance of the two bands is not known, whether this pattern is also observed in normal adult cell lines (other than tumoral and embryonic cells, as used here), or if one of the bands could correspond to the NAMPT-like protein. Even if expressed, such protein could be non-functional as determined by the analysis of the 3D structural model.

Three amino acids substitutions were evaluated. Concerning the first substitution, and as shown in figure 25, phenylalanine is an aromatic amino acid, contrary to valine. Both amino acids are hydrophobic and non-polar, however valine is smaller and with this substitution the protein loses one polar contact with water.

Concerning the second one, and as shown in figure 27, the amino acids are quite different, in their chemical properties. Isoleucine is hydrophobic and asparagine is a polar amino acid. This modification results in the gain of polar contacts Y29 e L193.

Both these substitution are predicted to be damaging to the protein, however the most dramatic is the third substitution (figure 29 and 30), which involves a residue from the active site. [66]

In order to fulfill its action, NAMPT must be phosphorylated in histidine 247 causing catalytic activation. The phosphorylation of histidine 247 results in a structural modification of the catalytic site, increasing affinity between the enzyme and the substrate. This catalytic activation leads to stabilization of NAMPT-PRPP complex which allows an efficient capture of NAM [67].

As shown in figure 30, if one of the modifications in NAMPT-like protein leads to the loss of the polar contact of D279 with histidine 247, the result could be a less active enzyme.

CONCLUSION AND FUTURE PERSPECTIVES

This is the first work on NAMPT and NAPRT from human tumor cell lines that integrates all the three levels of biological information – DNA, RNA and protein.

Several polymorphisms were detected in both genes, and all but one were already described in available databases of genetic variation from human populations. As future work, sequencing the complete genes could uncover additional mutations.

The results also show that both genes are expressed in tumor cell lines, however further work is needed to characterize differential expression patterns and the novel isoforms identified. As RNA expression not always correlates with protein expression, studies concerning the consequences of the mutations found at the protein level should be performed, and enzymatic or functional assays used to predict the role of the different isoforms.

Conclusions and Future Perspectives

What concerns the use of NAMPT and NAPRT in anti-tumor therapies, knowledge is still missing. Are metastatic tumors comparable to the non-metastatic tumors? Are the patterns found in renal or lung tumors comparable with lung metastasis from renal carcinoma, for example? The use of different cell lines for the same cancer type could address these questions. But it is premature to infer about the efficiency of NA in treatments with NAMPT inhibitors in specific tissues and/or tumors.

BIBLIOGRAPHY

1. Huawen Lin, A.L.K., Susan K. Dutcher, *Synthesizing and Salvaging NAD$^+$: Lessons learned from Chlamydomonas reinhardtii.* Plos Genetics, 2010. **Vol. 6**.
2. Riekelt H. Houtkooper, C.C., Ronald J. Wanders, and Johan Auwerx, *The Secret Life of NAD$^+$: An Old Metabolite Controlling New Metabolic Signaling Pathways.* Endocrine Reviews, 2010. **Vol. 31**: p. 194–223.
3. Mara Gallí, F.V.G., Anthony Rongvaux, Fabienne Andris, Oberdan Leo, *The Nicotinamide Phosphoribosyltransferase: A molecular link between Metabolism, Inflammation and Cancer.* Cancer Research, 2009. **70(1)**: p. 8-11.
4. Antje Garten, S.P., Antje Körner, Schin-ichiro Imai and Wieland Kiess, *Nampt: linking NAD biology, metabolism and cancer.* Cell Press, 2008. **Vol. 20**: p. 130-138.
5. Peter Belenky, K.L.B.a.C.B., *NAD+ metabolism in health and disease.* Trends in Biochemical Sciences, 2006. **Volume 32** p. 12-19.
6. Nadine Pollak, C.D.a.M.Z., *The power to reduce: pyridine nucleotides – small molecules with a multitude of functions.* Biochemical Society, 2007. **402(2)**: p. 205-218.
7. Bürkle, A., *Poly(ADP-ribose) - The most elaborate metabolite of NAD+*. The FEBS Journal, 2005. **Vol 272**: p. 4576–4589.

Bibliography

8. Pawlikowska, L., *Extracelular Synthesis of cADP-ribose from nicotinamide-adenine dinucleotide by rat cortical astrocytes in culture* Journal of Neuroscience, 1996. **16(17)** p. 5372-5381
9. Shin-ichiro Imai, C.M.A., Matt Kaeberlein & Leonard Guarente, *Transcriptional silencing and longevity protein Sir2 is an NAD-dependent histone deacetylase.* Nature, 2000. **Vol. 403(6771)**: p. 795-800.
10. Csaba Szabo, P.P., Raymond A. Swanson, *Novel modulators of poly(ADP-ribose) polymerase.* Trends in Pharmacological Sciences, 2006. **Vol. 27**: p. 626-630.
11. Lászlo Virág, C.S., *The Therapeutic Potential of Poly(ADP-Ribose) Polymerase Inhibitors.* Pharmacological Reviews, 2002. **Vol. 54(3)**: p. 375-429.
12. Fabio Malavasi, S.D., *Evolution and Function of the ADP Ribosyl Cyclase/CD38 Gene Family in Physiology and Pathology.* American Physiological Society, 2008. **Vol. 88**: p. 841–886.
13. Anthony A. Sauve, C., Vern L. Schramm, and Jef D. Boeke, *The Biochemistry of Sirtuins.* Annual Review of Biochemistry 2006. **Vol. 75**: p. 435-465.
14. Takashi Nakagawa, L.G., *Sirtuins at a glance.* Journal of Cell Science, 2011. **Vol. 124**: p. 833-838.
15. Marcia C. Haigis, L.P.G., *Mammalian sirtuins - emerging roles in physiology, aging and calorie restriction* Genes & Development, 2012. **Vol. 20**: p. 2913-2921.
16. Lin SJ, D.P., Guarente L, *Requirement of NAD and SIR2 for life-span extension by calorie restriction in Saccharomyces cerevisiae*. . Science, 2000.
17. Rogina B, H.S., *Sir2 mediates longevity in the fly through a pathway related to calorie restriction.* Proc Natl Acad Sci USA 2004. **Vol. 101**: p. 15998-16003.
18. Tissenbaum HA, G.L., *Increased dosage of a sir-2 gene extends lifespan in Caenorhabditis elegans.* Nature, 2001. **Vol. 410(6825)**: p. 227-30.
19. Jianyuan Luo, A.Y.N., Shin-ichiro Imai, Delin Chen, Fei Su, Ariel Shiloh, Leonard Guarente, and Wei Gu, *Negative Control of p53 by Sir2 Promotes Cell Survival under Stress.* Cell, 2001. **Vol. 107**: p. 137–148.
20. G. Magni, A.A., M. Emanuelli, G. Orsomando, N. Raffaelli, S. Ruggieri, *Enzymology of NAD+ homeostasis in man.* Cellular and Molecular Life Sciences, 2004. **Vol. 61**: p. 19-34.
21. Tao Liu, P.Y.L.a.G.M.M., *The critical role of the class III Histone Deacetylase SIRT1 in cancer.* American Association for Cancer Research, 2009. **Vol. 69**: p. 1702-1705.
22. Guarente, G.D.a.L., *Aging and disease: connections to sirtuins.* Aging Cell, 2010. **Vol. 9**: p. 285–290.
23. Jingjie Yi, J.L., *SIRT1 and p53, effect on cancer, senescence and beyond.* Biochimica et Biophysica Acta, 2010. **Vol. 1804**: p. 1684–1689.
24. Ron Firestein., G.B., Shaday Michan, Philipp Oberdoerffer, Leonard P. Guarente, David A. Sinclair, *The SIRT1 Deacetylase Suppresses Intestinal Tumorigenesis and Colon Cancer Growth.* Plos One, 2008. **Vol. 3(4)**.
25. Pawel Bieganowski, C.B., *Discoveries of Nicotinamide Riboside as a Nutrient and Conserved NRK Genes Establish a Preiss-Handler Independent Route to NAD^+ in Fungi and Humans.* Cell Press, 2004. **Vol. 117**: p. 495-502.
26. Jennifer Sporty, S.-J.L., Michiko Kato, Ted Ognibene, Benjamin Stewart, Ken Turteltaub, Graham Bench, *Quantitation of NAD^+ biosynthesis from the salvage*

Bibliography

pathway in Saccharomyces cerevisiae. Wiley InterScience, 2009. **Vol. 26(7)**: p. 363-9.

27. Peter Belenky, F.G.R., Katrina L. Bogan, Julie M. McClure, Jeffrey S. Smith, and Charles Brenner, *Nicotinamide Riboside Promotes Sir2 Silencing and Extends Lifespan via Nrk and Urh1/Pnp1/Meu1 Pathways to NAD+*. Cell 2007. **Vol. 129**: p. 473-484.
28. Lucia Galassin, M.D.S., Lucia Brunetti, Giuseppe Orsomando, Adolfo Amici, Silverio Ruggieri, Giulio Magni, *Characterization of human nicotinate phosphoribosyltransferase: Kinetic studies, structure prediction and functional analysis by site-directed mutagenesis.* Biochimie, 2011.
29. Wolfram Tempel, W.M.R., Katrina L. Bogan, Peter Belenky, Marzena Wojcik, Heather F. Seidle, Lyudmila Nedyalkova, Tianle Yang, Anthony A. Sauve, Hee-Won Park, Charles Brenner, *Nicotinamide Riboside Kinase Structures Reveal New Pathways to NAD.* Plos Biology, 2007. **Vol. 5**: p. 2220-2230.
30. Kevin J. Bitterman, R.M.A., Haim Y. Cohen, Magda Latorre-Esteves, David A. Sinclair, *Inhibition of Silencing and Accelerated Aging by Nicotinamide, a Putative Negative Regulator of Yeast Sir2 and Human SIRT1.* The Journal of Biological Chemistry, 2002. **Vol. 277**: p. 45099–45107.
31. Kraus, T.Z.a.W.L., *SIRT1-dependent Regulation of Chromatin and Transcription: Linking NAD+ Metabolism and Signaling to the Control of Cellular Functions.* Biochimica et Biophysica Acta, 2010.
32. Tie-qiang Bi, X.-m.C., *Nampt/PBEF/visfatin and cancer.* Cancer Biology & Therapy, 2010. **Vol. 10(2)**: p. 119-25.
33. Ryo Takahashi, S.N., Takashi Nakazawa,, *Structure and reaction mechanism of human nicotinamide phosphoribosyltransferase.* The Journal of Biochemistry, 2009. **Volume 147**: p. 95-107.
34. Ryo Takahashi, S.N., Takashi Nakazawa,, *Crystallization of human nicotinamide phosphoribosyltransferase.* Crystallization Communications, 2007. **Vol. 63(5)**: p. 375-377.
35. Imai, S.-i., *Nicotinamide phosphoribosyltransferase (Nampt): A link between NAD biology, metabolism, and diseases.* Current Pharmaceutical Design, 2009. **Vol. 15**: p. 20-28.
36. Che, T.-q.B.a.X.-m., *Nampt/PBEF/visfatin and cancer.* Cancer Biology & Therapy, 2010.
37. Li Qin Zhang, D.P.H., and Shui Qing Ye, *Nicotinamide Phosphoribosyltransferase in Human Diseases.* Journal of Bioanalysis and Biomedicine, 2011.
38. Nobumasa Hara, K.Y., Tomoko Shibata, Harumi Osago, Tatsuya Hashimoto and Mikako Tsuchiya, *Elevation of cellular NAD levels by nicotinic acid and involvement of nicotinic acid phosphoribosyltransferase in Human cells.* Journal of Biological Chemistry, 2007. **Vol. 282**: p. 24574–24582.
39. Joshua S. Chappie, e.a., *The Structure of a Eukaryotic Nicotinic Acid Phosphoribosyltransferase Reveals Structural Heterogeneity among Type II PRTases.* Structure, 2005. **Vol. 13**: p. 1385–1396.
40. Hisayuki Kato, E.I., Wei Shi, Nehad M. Alajez, Shijun Yue, Carolina Lee, Norman Chan, Nirmal Bhogal, Carla L. Coackley, Doug Vines, David Green, John Waldron, Patrick Gullane, Rob Bristow, and Fei-Fei Liu, *Efficacy of Combining GMX1777 with Radiation Therapy for Human Head and Neck Carcinoma.* Clinical Cancer Research, 2010. **Vol. 16**: p. 898-911.

Bibliography

41. Douglas Hanahan, R.A.W., *Hallmarks of Cancer: The Next Generation.* Elsevier, 2011. **Vol. 144(5)**: p. 646-674.
42. Matthew G. Vander Heiden, L.C.C., Craig B. Thompson, *Understanding the Warburg Effect: The Metabolic Requirements of Cell Proliferation.* Science, 2009. **Vol. 324**: p. 1029-1033.
43. P. Sreekanth Reddy, S.U., Balaram Thota, Ashwani Tandon, *PBEF1/NAmPRTase/Visfatin - A potential malignant astrocytoma/glioblastoma serum marker with prognostic value.* Cancer Biology & Therapy, 2008. **Vol. 7(5)** p. 663-668.
44. Uffe H Olesen, N.H.a.M.S., *Expression patterns of nicotinamide phosphoribosyltransferase and nicotinic acid phosphoribosyltransferase in human malignant~ lymphomas.* APMIS, 2011. **Vol. 119(4-5)**: p. 296-303.
45. Rodney E Shackelford, M.M.B., Domenico Coppola, and Ardeshir Hakam, *Over-expression of nicotinamide phosphoribosyltransferase in ovarian cancers.* Int J Clin Exp Pathol, 2010. **Vol. 3(5)**: p. 522-527.
46. Takako Eguchi Nakajima, e.a., *Adipocytokines as new promising markers of colorectal tumors: Adiponectin for colorectal adenoma, and resistin and visfatin for colorectal cancer.* Cancer Science, 2010. **Vol. 101**: p. 1286–1291.
47. Uffe H Olesen, J.G.P., Antje Garten, Wieland Kiess, Jun Yoshino, Shin-Ichiro Imai, Mette K Christensen, Peter Fristrup, Annemette V Thougaard, Fredrik Björklin, Peter B Jensen, Søren J Nielsen, Maxwell Sehested, *Target enzyme mutations are the molecular basis for resistance towards pharmacological inhibition of nicotinamide phosphoribosyltransferase.* BioMed Central, 2010. **Vol. 10**: p. 677-690.
48. Nagasuma Chandra, R.B., Eshita Sharma, P Sreekanthreddy, Kumaravel Somasundaram, *Virtual screening, identification and experimental testing of novel inhibitors of PBEF1/Visfatin/ NMPRTase for glioma therapy.* Journal of Clinical Bioinformatics, 2011. **1**.
49. Heldin NE, G.B., Claesson-Welsh L, Hammacher A, Mark J, Heldin CH, Westermark B. , *Aberrant expression of receptors for platelet-derived growth factor in an anaplastic thyroid carcinoma cell line.* Proc Natl Acad Sci U S A., 1988. **Vol. 85**: p. 9302-9306.
50. Chen TR, D.C., McGuire LJ, Macy ML, Hay RJ, *DLD-1 and HCT-15 cell lines derived separately from colorectal carcinomas have totally different chromosome changes but the same genetic origin.* Cancer Genet. Cytogenet, 1995. **81(2)**: p. 103-108.
51. Hoshi H, M.W., *Brain- and liver cell-derived factors are required for growth of human endothelial cells in serum-free culture.* Proc. Natl. Acad. Sci. USA, 1984. **Vol. 81**: p. 6413-6417.
52. Lanotte, M., Martin-Thouvenin,V., Najman,S., Balerini,P., Valensi,F. & Berger,R, *NB4, a maturation inducible cell line with t(15;17) marker isolated from a human acute promyelocytic leukemia (M3).* Blood, 1991. **Vol. 77(5)**: p. 1080-1086.
53. Gallagher R, e.a., *Characterization of the continuous, differentiating myeloid cell line (HL-60) from a patient with acute promyelocytic leukemia.* Blood, 1979. **Vol. 54**: p. 713-733.
54. Drummond AJ, A.B., Buxton S, Cheung M, Cooper A, Heled J, Kearse M, Moir R, Stones-Havas S, Sturrock S, Thierer T, Wilson A, *Geneious v5.5* http://www.geneious.com, 2011.

Bibliography

55. Blundell, A.S.a.T.L., *Comparative protein modelling by satisfaction of spatial restraints.* J. Mol. Biol., 1993. **Vol. 234(3)**: p. 779-815.
56. Schrödinger, *The PyMOL Molecular Graphics System.* Version 1.2r3pre.
57. Sippl, M.J., *Recognition of Errors in Three-Dimensional Structures of Protein.* Proteins, 1993. **Vol. 17(4)**: p. 355-62.
58. Sippl, W., *ProSA-web: interactive web service for the recognition of errors in three-dimensional structures of proteins.* Nucleic Acids Research, 2007. **Vol. 35**: p. Web Server issue W407-W410.
59. Ramensky V, B.P., Sunyaev S., *Human non-synonymous SNPs: server and survey.* Nucleic Acids Res., 2002. **Vol. 30(17)** p. 3894-3900.
60. Watson M, R.A., Bélec L, Billot X, Marcellus R, Bédard D, Bernier C, Branchaud S, Chan H, Dairi K, Gilbert K, Goulet D, Gratton MO, Isakau H, Jang A, Khadir A., *The small molecule GMX1778 is a potent inhibitor of NAD+ biosynthesis: strategy for enhanced therapy in nicotinic acid phosphoribosyltransferase 1-deficient tumors.* Mol Cell Biol, 2009. **Vol. 29** p. 5872-5888
61. Venables, J.P., *Aberrant and Alternative Splicing in Cancer.* Cancer Research, 2004. **Vol. 64**: p. 7647-7654.
62. Zane Kalnina, P.Z., Aija Liné, *Alterations of Pre-mRNA Splicing in Cancer.* Genes, Chromosomes and Cancer, 2005. **Vol. 42**: p. 342-357.
63. Gardner, L.B., *Nonsense mediated RNA decay regulation by cellular stress: implications for tumorigenesis.* Mol Cancer Res, 2010. **Vol. 8(3)** p. 295-308.
64. Sangeeta Chatterjee, J.K.P., *Role of 5'- and 3'-untranslated regions of mRNAs in human diseases.* Biology of the Cell, 2009. **Vol. 101 (5)**: p. 251-262.
65. Zuben E. Sauna, C.K.-S., *Understanding the contribution of synonymous mutations to human disease.* Nature Reviews Genetics, 2011. **Vol. 12**: p. 683-691.
66. Emmanuel S. Burgos, M.-C.H., Vern L. Schramm, *A phosphoenzyme mimic, overlapping catalytic sites and reaction coordinate motion for human NAMPT.* PNAS, 2009. **Vol. 106**: p. 13748-13753.
67. P.V. Krishna Pant, H.T., Erica J. Beilharz, et al., *Analysis of allelic differential expression in human white blood cells.* Genome Research, 2006. **Vol. 16**: p. 331-339.

Appendix

APPENDIX

Appendix

Figure 31 - Representation of concatenation obtained with primers to NAMPT cDNA

786-O:

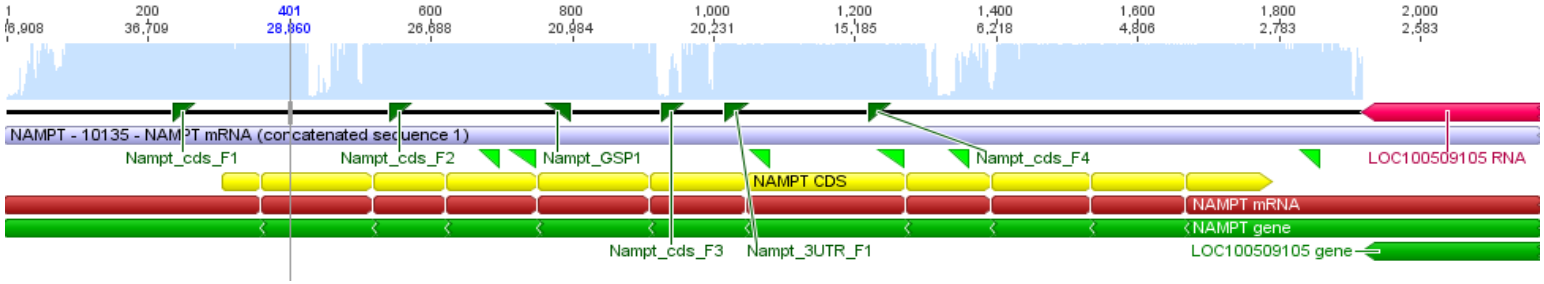

C643:

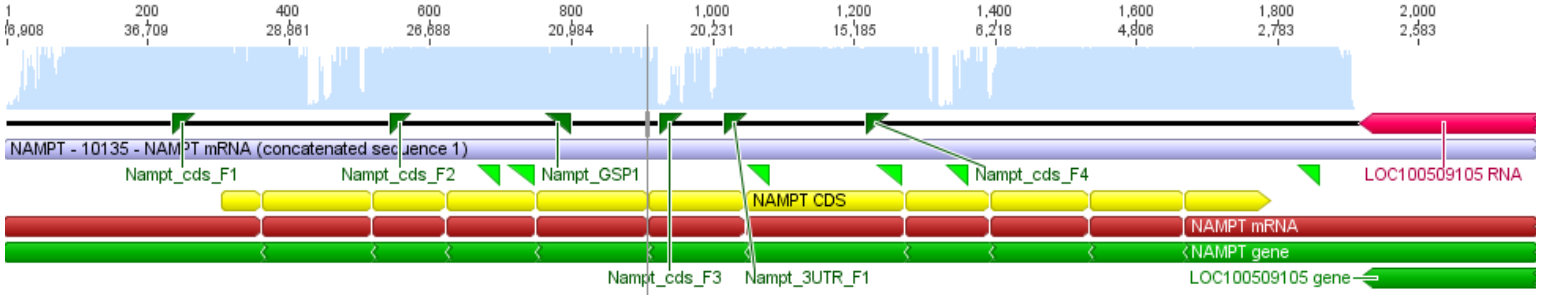

Appendix

Mel 202:

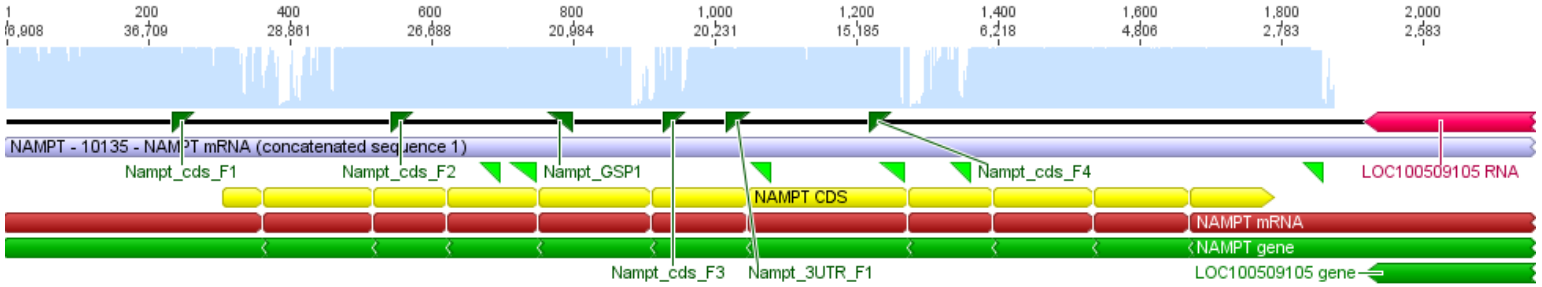

HUVEC-C:

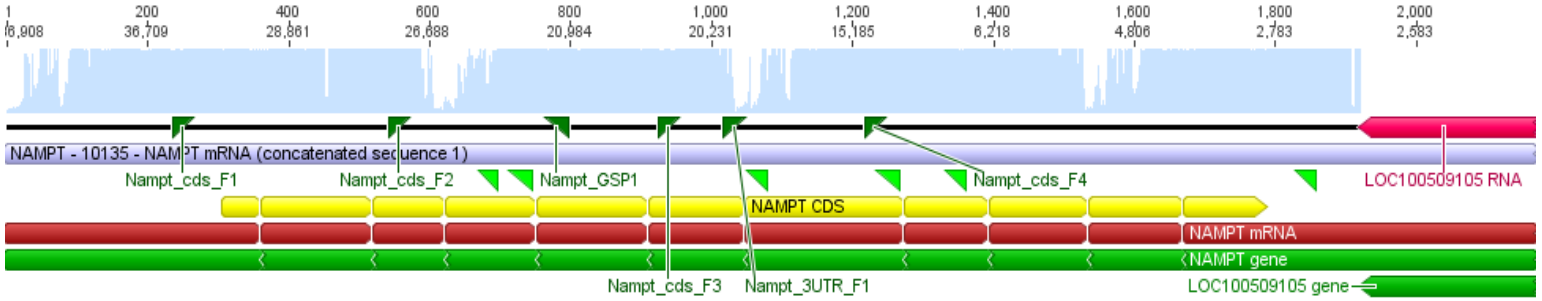

Hela:

Appendix

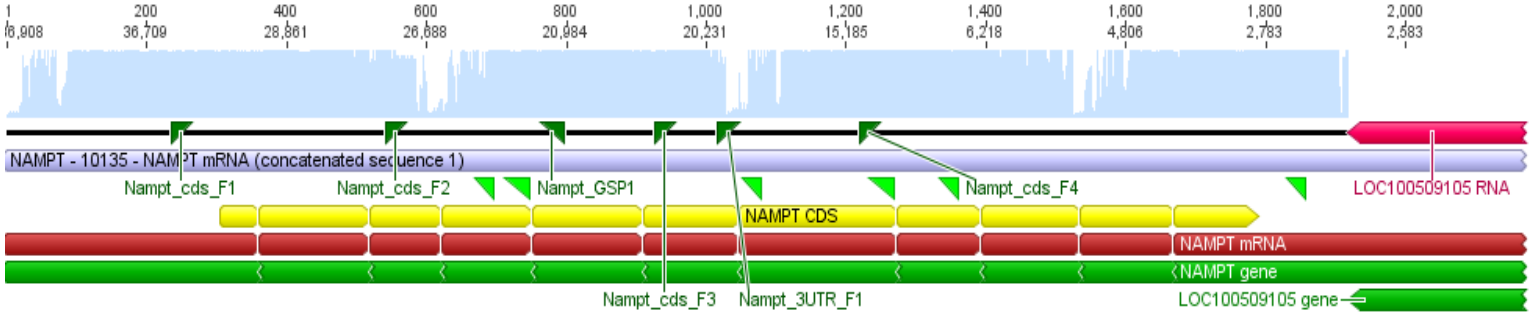

NB-4:

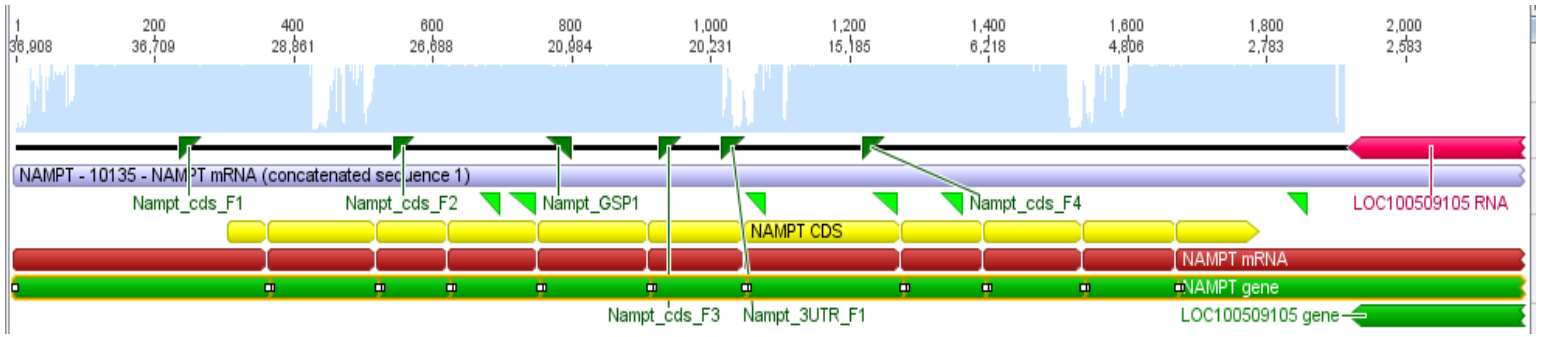

Appendix

HL-60:

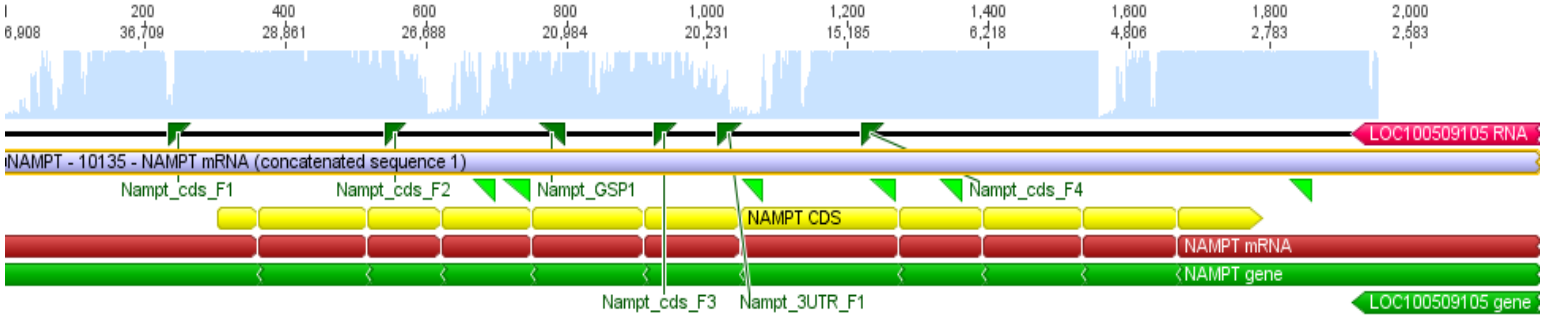

HCT-15:

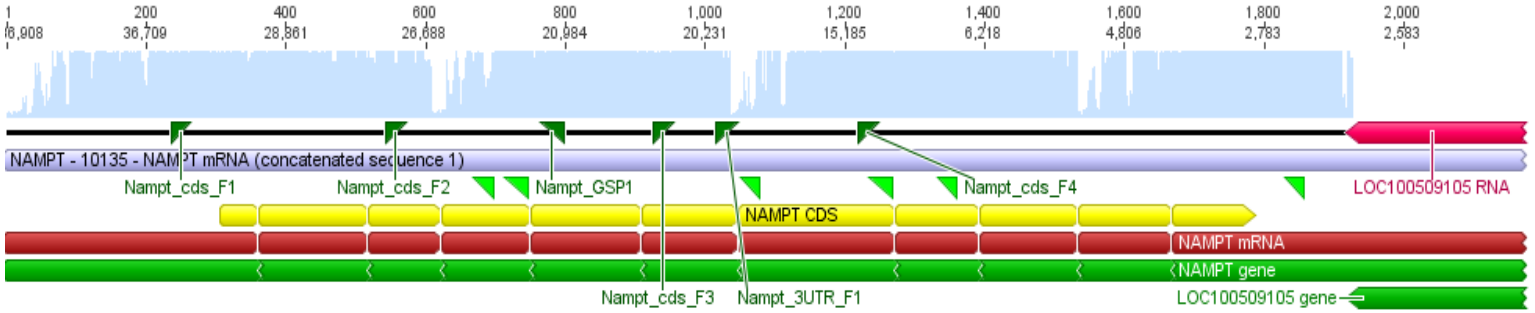

Appendix

A549:

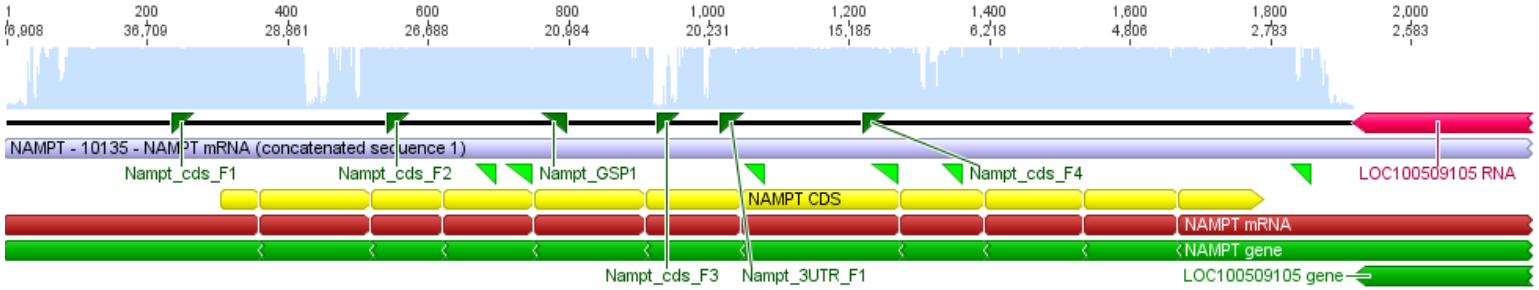

Figure 32 - Representation of the differences tested between NAMPT and NAMPT-like

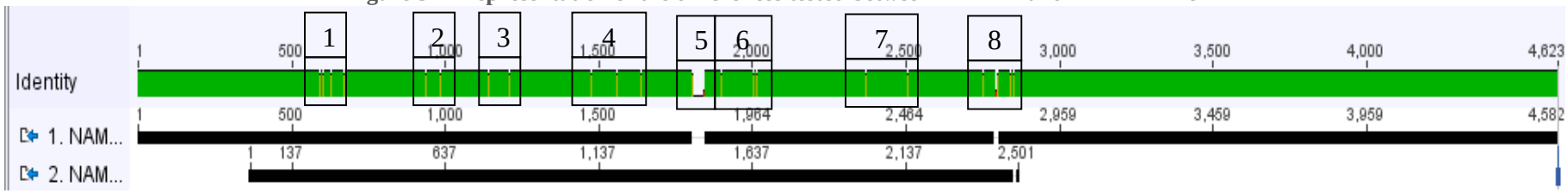

1.

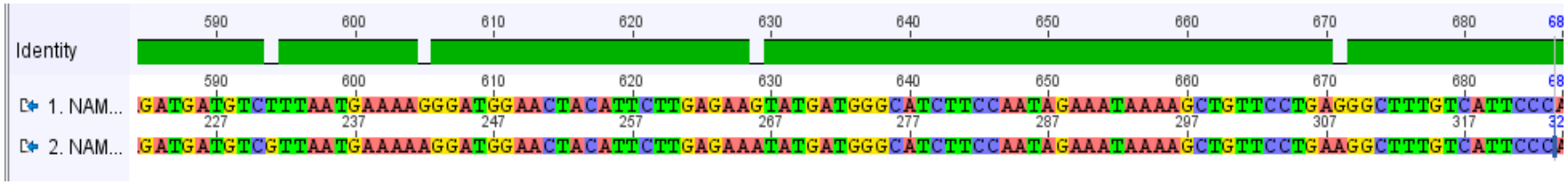

68

Appendix

2.

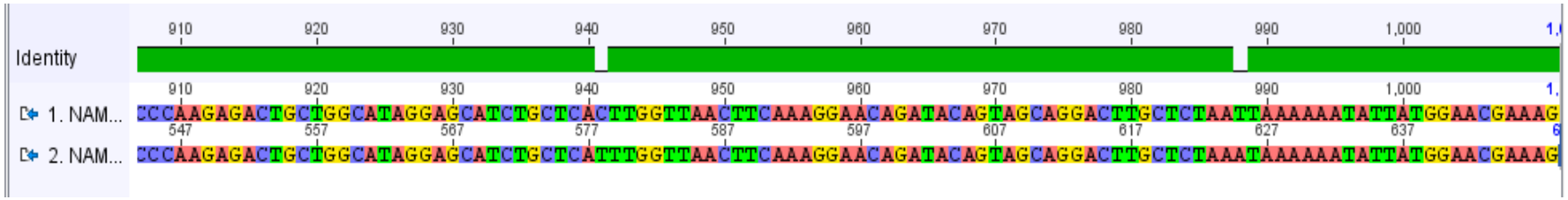

3.

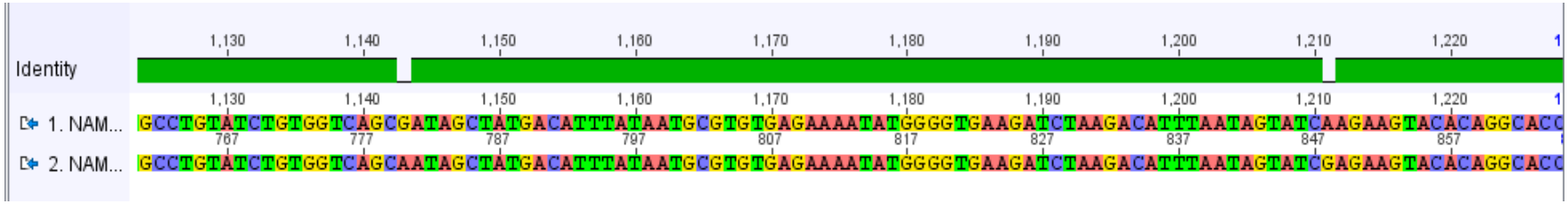

4.

5.

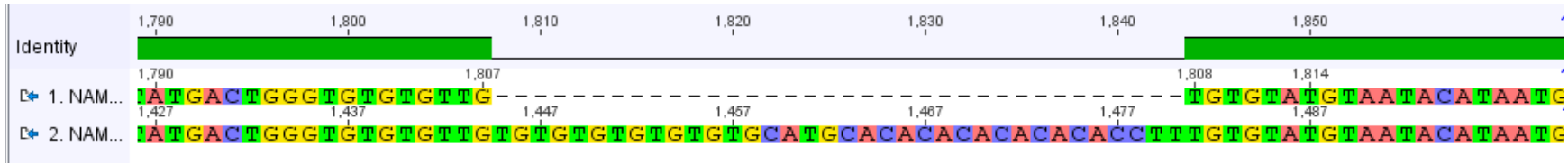

Appendix

6.

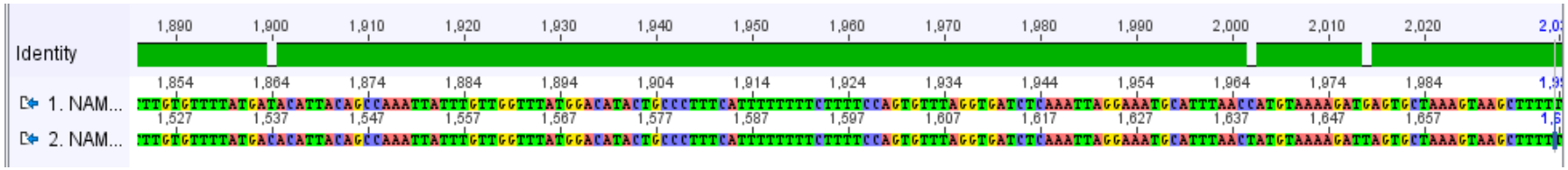

7.